coatings

MDPI

Review

Design of Icephobic Surfaces by Lowering Ice Adhesion Strength: A Mini Review

Zhiwei He [1,*], Yizhi Zhuo [2], Zhiliang Zhang [2] and Jianying He [2,*]

[1] Center for Advanced Optoelectronic Materials, Anti-Icing Materials (AIM) Lab, College of Materials and Environmental Engineering, Hangzhou Dianzi University, Hangzhou 310018, China
[2] NTNU Nanomechanical Lab, Department of Structural Engineering, Norwegian University of Science and Technology (NTNU), 7491 Trondheim, Norway; yizhi.zhuo@ntnu.no (Y.Z.); zhiliang.zhang@ntnu.no (Z.Z.)
* Correspondence: zhiwei.he@hdu.edu.cn (Z.H.); jianying.he@ntnu.no (J.H.)

Abstract: Ice accretion can lead to severe consequences in daily life and sometimes catastrophic events. To mitigate the hazard of icing, passive icephobic surfaces have drawn widespread attentions because of their abilities in repelling incoming water droplets, suppressing ice nucleation and/or lowering ice adhesion strength. As time elapses and temperature lowers sufficiently, ice accretion becomes inevitable, and a realistic roadmap to surface icephobicity for various outdoor anti-icing applications is to live with ice but with the lowest ice adhesion strength. In this review, surfaces with icephobicity are critically categorized into smooth surfaces, textured surfaces, slippery surfaces and sub-surface textured surfaces, and discussed in terms of theoretical limit, current status and perspectives. Particular attention is paid to multiple passive anti-icing strategies combined approaches as proposed on the basis of icephobic surfaces. Correlating the current strategies with one another will promote understanding of the key parameters in lowering ice adhesion strength. Finally, we provide remarks on the rational design of state-of-the-art icephobic surfaces with low ice adhesion strength.

Keywords: superhydrophobic surfaces; slippery surfaces; ice adhesion strength; anti-icing; macro-crack initiators (MACI)

Citation: He, Z.; Zhuo, Y.; Zhang, Z.; He, J. Design of Icephobic Surfaces by Lowering Ice Adhesion Strength: A Mini Review. *Coatings* **2021**, *11*, 1343. https://doi.org/10.3390/coatings11111343

Academic Editor: Carlo Antonini

Received: 29 September 2021
Accepted: 29 October 2021
Published: 1 November 2021

1. Introduction

Undesired ice accretion on exposed surfaces becomes a severe issue to the safety operation of instruments and facilities, including aircrafts, wind turbines, solar panels, power lines, vehicles, ships and offshore oil platform [1]. The accretion of ice not only brings inconvenience to our daily life but also causes enormous economic loss each year, through, for example, frozen rain (Southern China, 2008), snow storms (Northeast USA, 2014) and aircraft accidents (Colgan Air Flight 3407, 2009). To mitigate icing problems, active de-icing methods have been widely employed with great efforts, such as mechanical vibration, thermal heating and chemical fluid spray [2]. However, the above de-icing methods suffer from having low efficiency and being energy-intensive and environmentally unfriendly [3]. Given frequent outdoor icing occurrence, these methods are expensive and suboptimal in practical applications.

An alternative approach is to introduce passive icephobic surfaces that require at least one of the following abilities: (1) to repel incoming water droplets, (2) to delay ice nucleation and (3) to lower ice-solid adhesion strength [4,5]. Bio-inspired from lotus leaves, superhydrophobic surfaces (SHSs) (contact angle >150° and contact angle hysteresis <10°) can easily shed off water droplets because of their hierarchical structures and low surface energy, showing excellent water repellency (Figure 1a) [6–10]. When SHSs still keep the ability of repelling water droplets below 0 °C, these SHSs can be called icephobic surfaces. In the meantime, SHSs can delay ice nucleation because of their low

surface energy barrier and high thermal barrier (i.e., trapped air among hierarchical structures). For example, Guo et al. decorated ZnO nanohairs on micro-structured stainless-steel plates, and a water droplet (7 μL) lasted for a long delay time of 7220 s for ice formation [11]. From the view of ice nucleation, SHSs show much longer ice nucleation time than ordinary surfaces, showing the property of icephobicity below 0 °C. When a water droplet in the Cassie–Baxter state is completely frozen, micro-crack initiators can facilitate the fracture of ice at the interface [12]. Yet, SHSs can lose their water repellency under high vapor pressure, and water droplets on SHSs change from the Cassie–Baxter state (i.e., air is trapped among hierarchical structures and liquid only contacts at top of hierarchical structures) to the Wenzel state (i.e., hierarchical structures are fully wetted by liquid and no air is trapped among hierarchical structures) (or the mixture state) (Figure 1b,c) where "Wenzel ice" (i.e., frozen water in Wenzel state) begins to interlock with hierarchical structures below 0 °C [12]. As time elapses and temperature lowers sufficiently, ice accretion becomes inevitable, and thus a realistic roadmap to surface icephobicity for various outdoor anti-icing applications is to live with ice but with the lowest ice adhesion strength such that ice can spontaneously shed off from exposed surfaces by its own weight, vibration or natural wind [2,13,14]. Recently, many reviews have been reported on icephobic surfaces from the viewpoint of bio-inspired [14,15], durable [16], dynamic [17], elastic [18,19], superhydrophobic [20,21] and slippery surfaces [22,23], providing good insights into surface icephobicity in terms of ice repellency, delay of ice nucleation and/or low ice adhesion, respectively. However, there are only a few review papers focusing on lowering ice adhesion strength, and they lack a summary on the rational design of icephobic surfaces through lowering ice adhesion strength as well as their corresponding mechanisms.

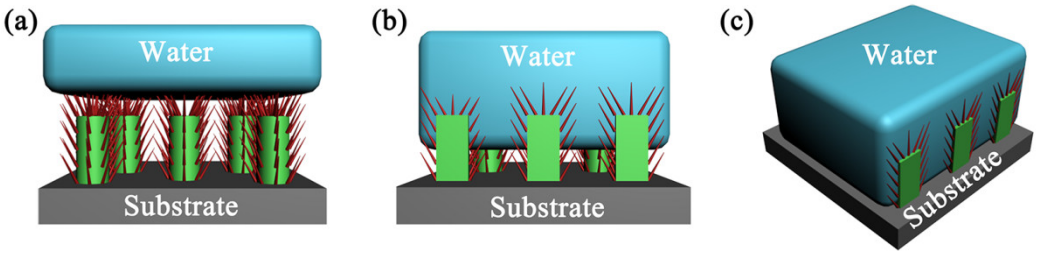

Figure 1. Three wetting behaviors: (**a**) Cassie–Baxter state (i.e., water only contacts with atop of hierarchical structures); (**b**) mixture state between Cassie–Baxter state and Wenzel state; and (**c**) Wenzel state (i.e., completely wetted state, cross-sectional view).

Herein, based on the surface morphology and its anti-icing design principles, surfaces with icephobicity are categorized into smooth surfaces, textured surfaces, slippery surfaces and sub-surface textured surfaces (Figure 2). The working mechanism, current status, theoretical limit and perspectives of these surfaces are discussed. The possibility of combining multiple passive anti-icing strategies is investigated to achieve ice adhesion strength as lowest as possible, promoting an understanding of the key parameters in lowering ice adhesion strength. Finally, we provide remarks on state-of-the-art of icephobic surfaces with low ice adhesion in future.

Figure 2. Strategies towards designing icephobic surfaces by lowering ice adhesion strength can be roughly divided into four types via surface properties: smooth surfaces, textured surface (i.e., hierarchical hydrophobic surfaces or SHSs), slippery surfaces, and sub-surface textured surfaces.

2. Strategies towards Designing of Icephobic Surfaces by Lowering Ice Adhesion Strength

Generally, icephobic surfaces can be defined by ice adhesion strength (τ_{ice}) below 100 kPa [4,24]. According to the surface properties (i.e., surface chemistry, surface topographies and sub-surface structures), icephobic surfaces can be categorized into smooth surfaces, textured surfaces, slippery surfaces and sub-surface textured surfaces. When comparing the icephobic property of above surfaces via ice adhesion strength, test methods and conditions should be comparable. Factors that influence ice adhesion strength include test method (e.g., horizontal shear, vertical shear, centrifugal shear and tensile strength) [25], test temperature (−30~0 °C) [25], characterization instrument [5], procedure of ice formation [25–27], type of ice (i.e., precipitation ice, in-cloud ice and bulk water ice) [26], size of ice [28], type of surface (surface chemistry, surface topography, elastic modulus and sub-surface structure) [29], loading rate [30] and failure behavior [25]. For all the data of ice adhesion strength discussed in this paper (Figure 3), the failure behavior refers to the adhesive failure between the substrate and ice but not the cohesive failure within ice or substrate. The instrument is usually test-method-dependent, while the type of ice depends on the icing conditions (i.e., temperature, humidity and vapor pressure). The size of ice (i.e., usually refer to the length of ice) influences ice adhesion on a chosen surface [28,29], whereas the overwhelming majority of the studies on ice adhesion strength do not consider it. Thus, ice adhesion strength of above four types of icephobic surfaces from 162 journal papers has been summarized under the consideration of test method (e.g., horizontal shear, vertical shear, centrifugal shear and tensile strength) and temperature (−30 ~0 °C) (Figure 3). Up to now, there are no standards for the preparation of ice cubes and the testing methods of ice adhesion strength, which makes it difficult to directly compare ice adhesion strength by its value. Figure 3 provides an overview that ice adhesion strength can be compared for four types of surfaces under the same test temperature and evaluation method. In general, when test method and temperature are chosen, ice

adhesion strength should be comparable. In this section, four types of icephobic surfaces are discussed based on ice adhesion strength in terms of theoretical limitation, current status and perspectives.

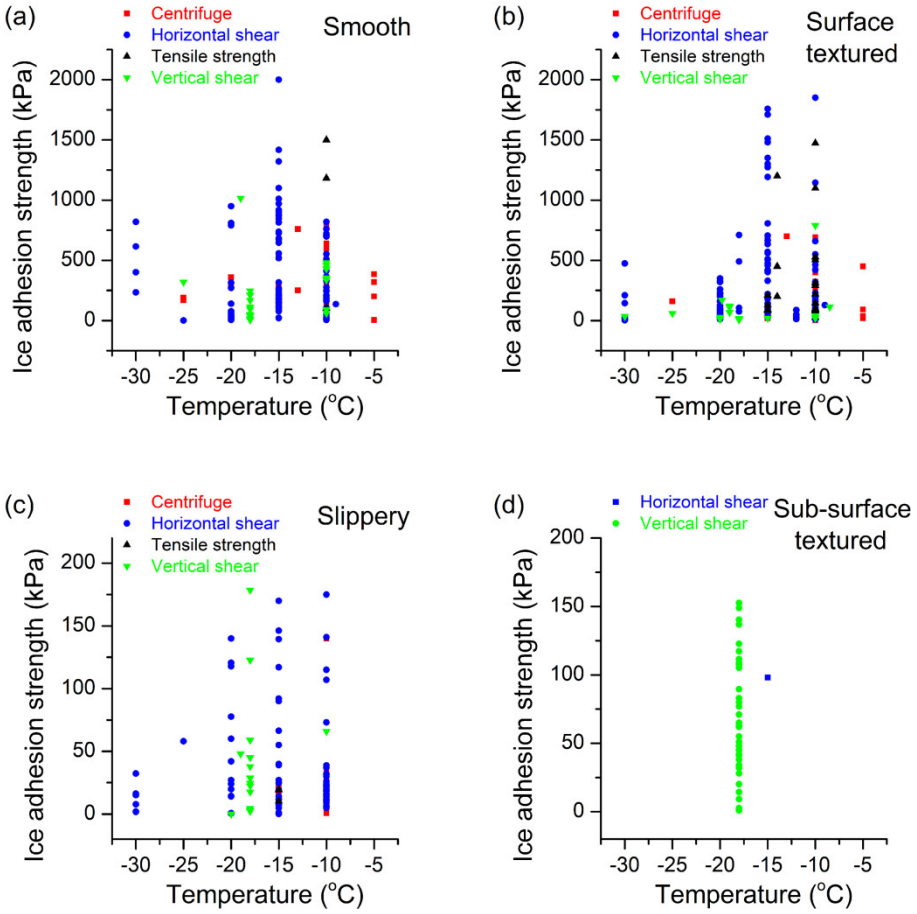

Figure 3. Ice adhesion strength plotted against temperature (i.e., range from 0 to −30 °C) by using different ice adhesion test methods (i.e., centrifuge, tensile, horizontal shear and vertical shear): (**a**) smooth surfaces, (**b**) textured surfaces, (**c**) slippery surfaces and (**d**) sub-surface textured surfaces. Data are collected from the literature [1,2,5,23,24,26,28,31–185].

2.1. Smooth Surfaces

The fabrication process of smooth surfaces is usually facile and cost-effective, which can be easily achieved by machining, depositing, molding, spraying, spin-coating, dip-coating and so on. Smooth surfaces are good candidates for surface icephobicity as long as ice adhesion strength of surfaces is less than 100 kPa [4]. Generally, ice adhesion strength of smooth solid surfaces is below 2 MPa (i.e., horizontal shear test), as shown in Figure 3 [1,4,5,13,24,41]. For example, ice adhesion strength of typical metallic surfaces is larger than 600 kPa (i.e., vertical shear test) [1,5]. For non-textured smooth surfaces with high elastic modulus, a theoretical lower limit for ice adhesion strength is about 150 kPa (i.e., horizontal shear test) [24]. Thus, most of smooth surfaces are not icephobic on the basis of the definition of icephobicity.

From the viewpoint of fracture mechanics, ice adhesion strength can be estimated by the following equation [13,186,187]:

$$\tau_c = \sqrt{E^* G / (\pi a \Lambda)} \quad (1)$$

where E^* is the apparent elastic modulus, G is the surface energy, a is the length of the interface crack and Λ is a non-dimensional constant determined by the geometric

configuration of the crack. According to the equation (1), ice adhesion strength can be reduced by decreasing elastic modulus for a chosen material surface. Thus, ice adhesion strength of smooth surfaces can be further reduced below 100 kPa by tuning elastic modulus and/or surface chemistry as suggested by the equation (1). For example, He et al. decreased elastic modulus and surface energy of polydimethylsiloxane (PDMS) based coatings by tuning the weight ratio of prepolymer and curing agent ranging from 10:1 to 10:10 and thus lowered ice adhesion strength (Figure 4a) [2]. Beemer et al. developed novel inexpensive, environmentally benign, non-corrosive PDMS gels that offer ultra-low adhesion to ice (τ_{ice} = 5.2 ± 0.4 kPa) as well as outstanding mechanical durability by reducing shear modulus of PDMS gels [41]. Moreover, He et al. investigated the correlation between ice adhesion strength and elastic modulus of 24 substrates and found that low elastic modulus of coatings did not guarantee low ice adhesion strength, while surfaces with low ice adhesion strength always show low elastic modulus [5]. In short, ice adhesion strength of coatings with low elastic modulus (i.e., elastomers and organogels) is determined by the failure mechanism of ice as well as the coating thickness.

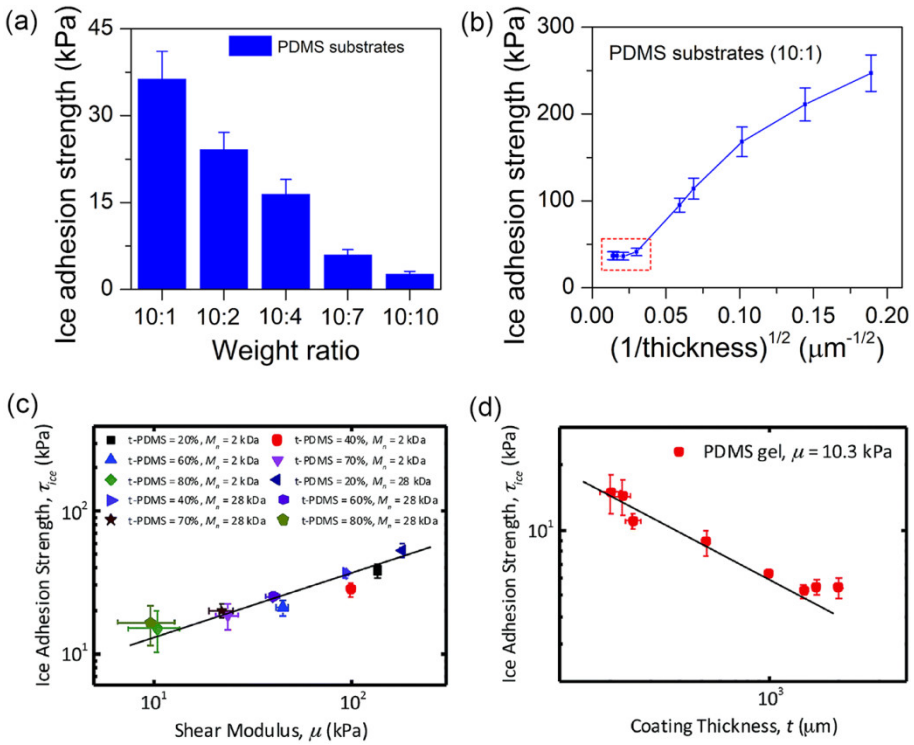

Figure 4. Ice adhesion strength at −18 °C plotted against (**a**) PDMS substrates and sandwich-like PDMS sponges with the weight ratio of prepolymer and curing agent ranging from 10:1 to 10:10; (**b**) correlation between ice adhesion strength and PDMS coating thickness in (**a**); (**c**) correlation between ice adhesion strength and shear modulus of PDMS gels; and (**d**) correlation between ice adhesion strength and coating thickness of PDMS gels in (**c**). Panel a and b reproduced with permission from Ref. [2], Copyright 2018, the Royal Society of Chemistry; panel c and d reproduced with permission from Ref. [41], Copyright 2016, the Royal Society of Chemistry.

The failure mechanism at the ice-substrate interface may depend on the size of ice, type of ice and flexibility of the smooth substrate [29]. The removal of ice occurs in a brittle manner for smooth surfaces with high elastic modulus, while ductile behavior occurs for highly elastic smooth surfaces because of surface deformations during the detachment of ice [29]. In the latter case, the ice interface usually behaves like that of a ductile material with little tendency to fracture when smooth surfaces are highly elastic [29]. For example, Beemer et al. reported that air-trapped cavity at the interface between ice and the PDMS gel surface propagated as a separation pulse and resulted in a stick slip motion, as shown in Figure 5a [41,188]. Chaudhury et al. demonstrated that the elastic instability led to the

development of interfacial cavities at the interface between glass and PDMS rubber such that it allowed localized deformations [189]. Irajizad et al. introduced stress-localized interfacial cavity between ice and organogel, thereby leading to the propagation of crack at the interface and achieving ice adhesion strength of 1 kPa, as shown in Figure 5b [143]. Moreover, the coating thickness is another factor that correlates with the ductile deformation and the wavelength of elastic instability, which are caused by the interfacial cavitation and subsequent minimization of the shear and longitudinal deformation energies of the elastic coating and thus influence ice adhesion strength [189,190]. For example, Chaudhury et al. considered the wavy segments as individual cracks during the detachment of ice, leading to the decrease of ice adhesion strength [189]. Wang et al. found that increasing the thickness of PDMS surfaces from 18 to 533 μm can reduce ice adhesion strength when removing a solid from an elastomeric substrate, as suggested by Kendell [53,191]:

$$P_c \propto \pi a^2 \sqrt{2w_a K / t} \quad (2)$$

where there is a correlation of the force (P_c) required to remove a rigid cylinder with work of adhesion (w_a), bulk modulus (K), thickness (t) and radius (a). Kendall's theory can be used for the removal of a rigid object from an elastic film in tensile mode, and there is also a relationship between tensile and shear modulus ($K_{tensile} = 3K_{shear}$) [53,192]. This correlation has been also verified by He et al. (that increasing coating thickness can reduce ice adhesion strength), and ice adhesion strength became stable when the thickness of PDMS substrate reached 4.8 mm, as shown in Figure 4b,d [2].

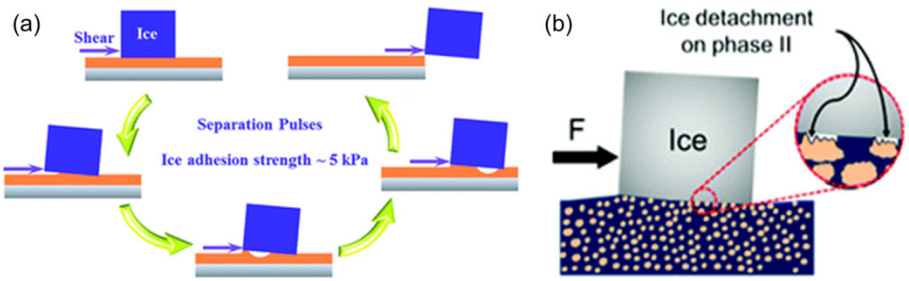

Figure 5. (**a**) Schematic illustrating the separation of ice from PDMS gels via separation pulses. During a horizontal shear, air can be trapped into air cavities, and these air cavities can be propagated via separation pulses; (**b**) stress-localized viscoelastic icephobic material consists of two phases: silicon elastomer (Phase I) and silicon-based organogel (Phase II). The crack forms at the coordinate of phase II with minimal forces. Panel (**a**) reproduced with permission from Ref. [41], Copyright 2016, the Royal Society of Chemistry; panel (**b**) reproduced with permission from Ref. [143], Copyright 2019, the Royal Society of Chemistry.

From the above discussion, we find that smooth elastic surfaces can be icephobic and even achieve extremely low ice adhesion strength by tuning surface chemistry, elastic modulus and surface thickness (Figures 3 and 4). Smooth elastic surfaces (i.e., elastomeric surfaces [2], organogels [41], hydrogels [193] and ionogels [194]) have attracted much attention because of low ice adhesion strength. For ice adhesion strength, elastic smooth surfaces may reach their own theoretical limits as affected by the coating thickness and the failure mechanism of ice (i.e., mechanism of separation pulses [41]) during a de-icing process. Thus, it is necessary to seek rational designs of anti-icing surfaces by the combination of multiple passive anti-icing strategies. For example, various kinds of elastic surfaces can be incorporated with polyelectrolytes, ions, salts and lubricants to enhance surface chemistry and interfacial slippage and thus lower ice adhesion strength because of potential synergistic effects of different anti-icing/de-icing strategies. Additionally, these elastic smooth surfaces can be rationally designed to be porous or sub-surface structured such that multi-scale crack initiators can be generated at the interface between ice and

substrate due to the stiffness inhomogeneity in both perpendicular and tangential directions.

2.2. Textured Surfaces

Textured surfaces with icephobicity usually contain hierarchical structures (i.e., hydrophobic surfaces and SHSs). Taking SHSs, for instance, some surfaces present excellent anti-icing behaviors, while others do not always show icephobicity [156,187,195–197]. This controversial issue arouses researchers' curiosity in SHS-based icephobicity all over the world. To explain this issue, three factors related to the variable surface icephobicity of SHSs are discussed as follows. The first factor is condensation. SHSs may lose superhydrophobicity (i.e., water repellency) in a highly humid environment (or supersaturation) [198–200]. Once the vapor pressure reaches critically high, or the droplets are too small, water droplets can slowly permeate hierarchical structures and fully wet the hierarchical structures of SHSs (Figure 6) [199]. For example, the lotus leaf surface became hydrophilic once it experienced water condensation [198]. The second factor is the inter-locking effect between ice and hierarchical structures of SHSs (Figure 6c). The water that has wetted the hierarchical structures of SHSs can freeze to ice, enveloping hierarchical structures at low temperatures (i.e., below 0 °C) [32,167], thereby leading to an increase of ice adhesion strength. The third factor is the sustainability of surface chemistry and hierarchical structures. The surface chemistry and the tips of hierarchical structures may be damaged during icing (i.e., water solidification) and/or de-icing (i.e., ice removal) cycles (Figure 6d) [156,201], resulting in the loss of surface superhydrophobicity. Besides, SHSs can also be applied for frost-resistant surfaces that can withstand several freeze-thaw cycles without damage when these surfaces suffer frost in the saturated state [202], which is different from the definition of icephobic surfaces.

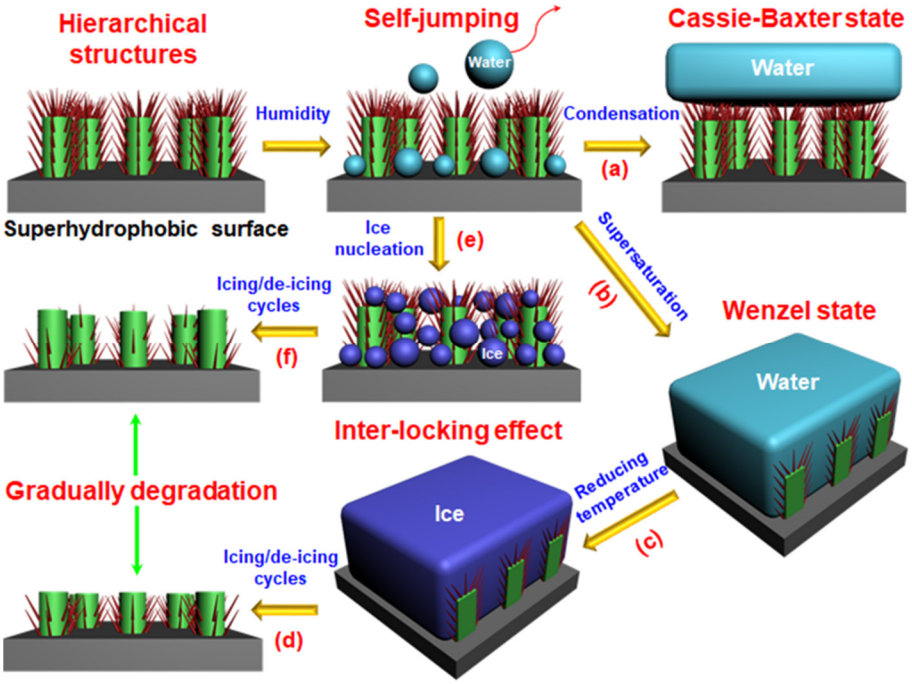

Figure 6. Overview of condensation on the superhydrophobic surface (SHS): (**a**) water remains at Cassie–Baxter state; (**b**) water completely wet hierarchical structures of SHS under supersaturation; (**c**) water in Wenzel state starts to freeze as temperature reduces, and then "Wenzel ice" forms; (**d**) de-icing of "Wenzel ice", and hierarchical structures and surface chemistry gradually degrades during icing/de-icing cycles; (**e**) icing of small water droplets among hierarchical structures at low temperature; and (**f**) small ice covered SHS during icing/de-icing cycles.

SHSs have been demonstrated to be water/ice-repellent in the outdoor applications [203–205]. For example, Cao et al. kept silica-based SHSs coated or uncoated aluminum plates under freezing rain, and they found SHSs showing excellent icephobicity [203]. Boinovich et al. carried out an outdoor test (i.e., a heavy snowfall at −3 °C) and showed the superhydrophobic coating being free of ice in comparison with untreated stainless steel [204]. In real long-term outdoor applications, SHSs will unavoidably lose water/ice-repellent properties as time elapses in cold and harsh environments. An alternative approach to achieving surface icephobicity is to lower ice adhesion strength [2,13]. During a de-icing process, the inter-locking effect between ice and hierarchical structures of SHSs cannot be ignored, which often causes the damage of hierarchical structures and thus induces an increase of ice adhesion strength (Figure 6). Actually, using SHSs as part of an an individual anti-icing strategy is not enough for the design of durable icephobic surfaces with low ice adhesion strength. Through integration with other passive anti-icing strategies (i.e., elastic substrates and lubricating layers), SHSs can alleviate the inter-locking effect, enhance robustness and lower ice adhesion strength. For example, Wang et al. reported that a flexible superhydrophobic coating showed a water and ice repellency at low temperatures (−20 °C) and high relatively humidity of 90% for up to three months [206]. Vasileiou et al. demonstrated that the collaborative effect of substrate flexibility and surface micro/nanotexture can enhance both icephobicity and the repellency of viscous droplets (i.e., typical of supercooled water) [207]. Wang et al. reported that a robust SHS with flexible micro-ratchet/ZnO nano-rods can recover its icephobicity after a freezing test [208]. Golovin et al. investigated an SHS with flexible PDMS-based micropillars and found its ice adhesion strength of 26 ± 3 kPa for 20 successive icing/de-icing cycles [24]. Barthwal et al. prepared robust and durable lubricating anti-icing coating by infusing silicone oil on superhydrophobic aluminum surfaces, and ice adhesion strength on this lubricating anti-icing coating was as low as 22 ± 5 kPa [44].

Although hydrophobic or superhydrophobic surfaces cannot be guaranteed as icephobic surfaces for a long time, researchers still try to find correlations between ice adhesion strength and room temperature characteristics, such as wettability, surface roughness, elastic modulus, hardness and water adhesion force [1,5]. Among these characteristics, the value of $(1 + \cos\theta_{rec})$ and water adhesion force have attracted much attention in recent years. For example, Mckinley and Cohen et al. found a linear correlation between ice adhesion strength and the value of $(1 + \cos\theta_{rec})$ in 2010 when ice adhesion strength of surfaces is larger than 150 kPa (Figure 7a) [1], but later in 2017 they found that this correlation become inaccurate for elastomeric surfaces (Figure 7b) [75]. This is because water contact angle only reflects surface chemistry of surfaces, while it cannot indicate elastic modulus of surfaces. Recently, He et al. found that water adhesion force correlates well with ice adhesion strength when ice adhesion strength is larger than 100 kPa (Figure 7c) [2,5]. Below 100 kPa, low ice adhesion strength is associated with low water adhesion force ranging from 160 to 315 μN (Figure 7c,d) [2,5]. The working process of water adhesion force is similar to that of ice detachment, and water adhesion force as well as ice adhesion strength can simultaneously reflect surface chemistry, elastic modulus and subsurface structures.

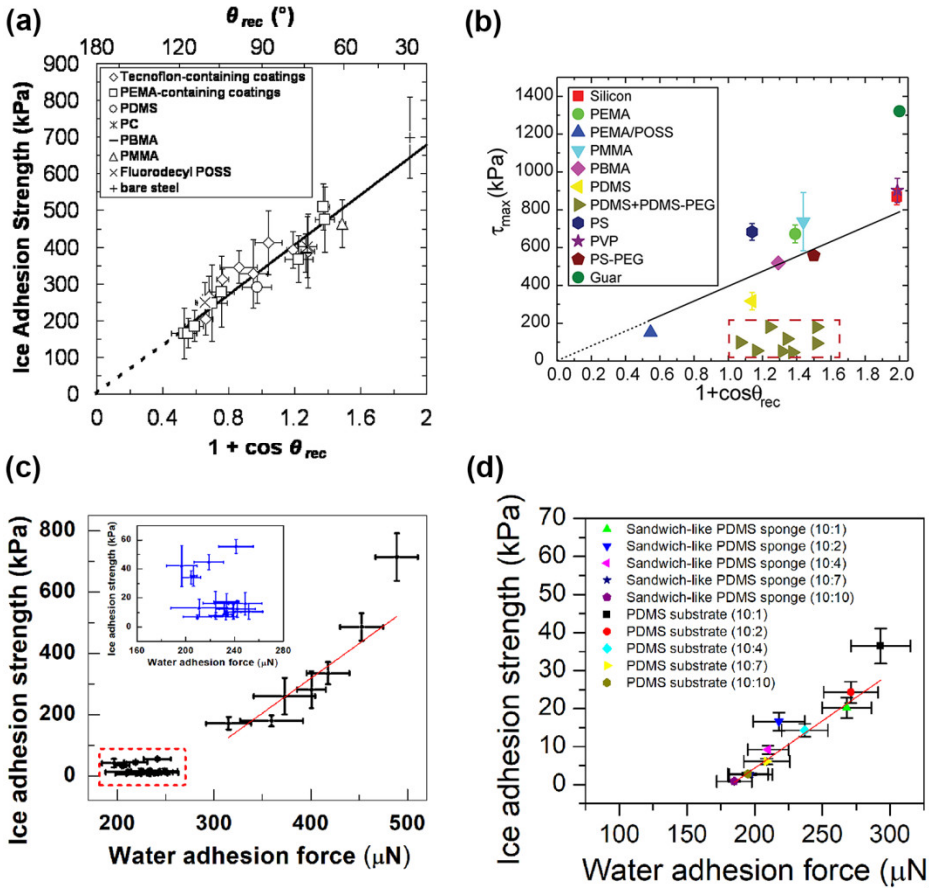

Figure 7. Correlations between ice adhesion strength and the value of (1 + cosθ_{rec}): (**a**) ice adhesion strength measured at −10 °C for bare steel and 21 different coatings; (**b**) ice adhesion strength measured at −15 °C for 17 different polymer coatings and a bare clean silicon wafer. Correlations between ice adhesion strength and water adhesion force (i.e., the water adhesion force was investigated by a Dynamic Contact Angle Tensiometer (DCAT11s, dataphysics) at room temperature): (**c**) 24 different coatings; and (**d**) 10 PDMS-based coatings. (**a**) Reproduced from Ref. [1] with permission, Copyright 2010 American Chemical Society; (**b**) reproduced from Ref. [75] with permission, Copyright 2017 American Chemical Society; (**c**) reproduced from Ref. [5] with permission, Copyright 2017 Springer Nature Publishing AG; and (**d**) reproduced from Ref. [2] with permission, Copyright 2018 the Royal Society of Chemistry.

In summary, surface icephobicity of SHSs can be easily maintained before ice formation occurs on SHSs. Once accumulated ice covers SHSs, ice adhesion strength can still be low if "Cassie ice" forms on the top of hierarchical structures of SHSs. For real outdoor applications, SHSs as an individual anti-icing approach may be suitable for short-term use, while they are not proper for a long-term use because superhydrophobicity will be gradually destroyed during icing/de-icing cycles. To cope with these drawbacks (i.e., inter-locking effect and degradation of surface chemistry and hierarchical structures) of SHSs, multiple passive anti-icing strategies need to be considered for incorporation with SHSs, including elastic/flexible substrates, sub-surface structures and lubricating layers, to provide robust SHSs with durable icephobicity.

2.3. Slippery Surfaces

Slippery surfaces with icephobicity usually refer to lubricating surfaces, such as organic lubricating layers and aqueous lubricating layers. Organic lubricating layers often contain sacrificial layers (e.g., oils, liquid paraffin, and perfluorinated fluids) that are immiscible with water [24,97,209]. Ice can be easily shed from these surfaces, but at the same time this depletes the organic lubricant. Aqueous lubricating layers consist of hygroscopic

polymers that can absorb water and form an interfacial non-frozen layer below 0 °C [38,75,76,185], working as a lubricating layer during a de-icing process. In this section, two kinds of lubricating surfaces with low ice adhesion strength will be discussed, and the possibility of organic lubricating and aqueous lubricating surfaces will be investigated for practical anti-icing applications.

2.3.1. Organic Lubricating Surfaces

Bio-inspired from Nepenthes pitcher plants, Aizenberg et al. reported a new lubricating surface named slippery liquid-infused porous surface (SLIPS) (Figure 8), which needs to meet three criteria: (1) the organic liquid firmly adhere within the porous substrate, (2) the substrate prefer to be wetted by the organic liquid rather than the external incoming liquid (i.e., water), and (3) the organic liquid and the external incoming liquid are immiscible [209]. This novel strategy opened a new avenue towards designing icephobic surfaces [70,96,150,152,177,210–220], showing low ice adhesion strength as described in Figure 3. From then on, more and more relevant researches have been explored. For example, Kim et al. impregnated a perfluorinated lubricant in polypyrrole-coated aluminum surface to obtain a SLIPS with ice adhesion strength (τ_{ice} = 15.6 ± 3.6 kPa) [152]. Zhang et al. fabricated a double-layered SLIPS coating on the AZ31 Mg alloy for anti-icing application [70]. Wang et al. obtained a SLIPS by infusing perfluorinated lubricants into a superhydrophobic coating consisting of SiO_2 nanoparticles and poly(methyl methacrylate), which functions remarkable anti-icing ability [211]. Wang et al. infused different lubricants into SHSs to form slippery icephobic surfaces with superior anti-icing properties [213]. Thus, SLIPS with low ice adhesion strength can be utilized in the anti-icing application.

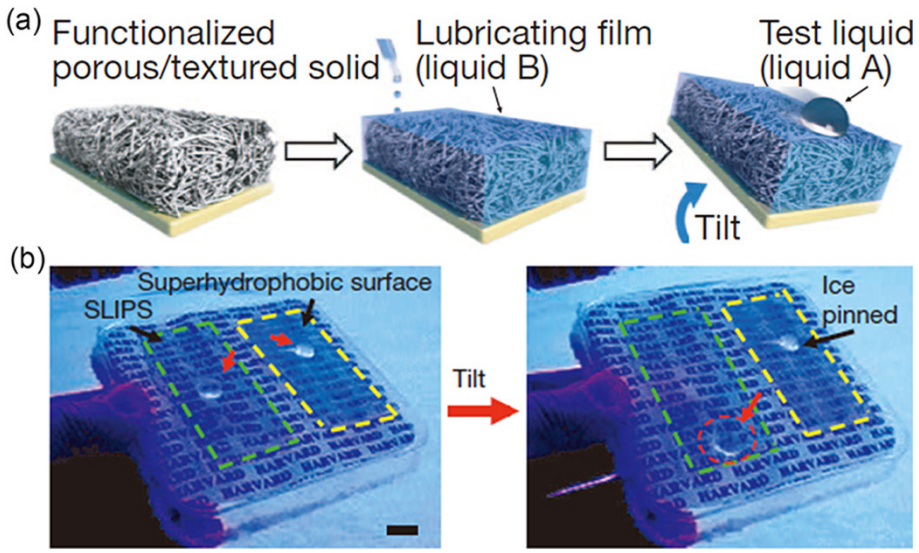

Figure 8. (**a**) Schematics showing the fabrication of a SLIPS by infiltrating a functionalized porous/textured solid with a low-surface energy, chemically inert liquid. (**b**) Ice mobility on a SLIPS (highlighted in green) compared to strong adhesion to an epoxy-resin-based nanostructured superhydrophobic surface (highlighted in yellow) when temperature and relative humidity were −4 °C and ~45%, respectively. (**a**, **b**) Reproduced with permission from [209], Copyright 2011 Macmillan Publishers Limited.

To understand the properties of organic lubricating layers, the stability of organic lubricant layers needs to be clarified. Preston et al. used a model as proposed by van Oss, Chaudhury and Good (vOCG) to predict unknown surface energies for an arbitrary system of solid and lubricant [221], and identified five criteria (Figure 9) for failure of an organic lubricant surface as follows [221]:

1) $S_{ld} \geq 0$, the lubricant spreads over the droplet; the droplet is cloaked,

2) $S_{dl} \geq 0$, the impinging fluid spreads over the lubricant and forms a film instead of discrete droplets,
3) $S_{ls} \leq -\gamma_l R$, the lubricant does not infuse in the hierarchical structures of substrate in the presence of the surrounding vapor,
4) $S_{ls(d)} \leq -\gamma_{dl} R$, the lubricant does not infuse in the hierarchical structures of substrate in the presence of the impinging fluid,
5) $\gamma_{dl} \leq 0$, the lubricant and the impinging fluid are miscible, where subscripts l, d, s refer to lubricant, impinging fluid and substrate, respectively, where S_{xy} represents the spreading parameter for x spreading over y, and $R = (r-1)(r-\phi)$ is a roughness factor calculated using the roughness (r) and the solid fraction (ϕ), and is 0 for a flat substrate and 1 for a very rough substrate [221,222]. Thus, these five criteria need to be considered when a water droplet is on slippery surfaces at low temperature (i.e., before ice nucleation).

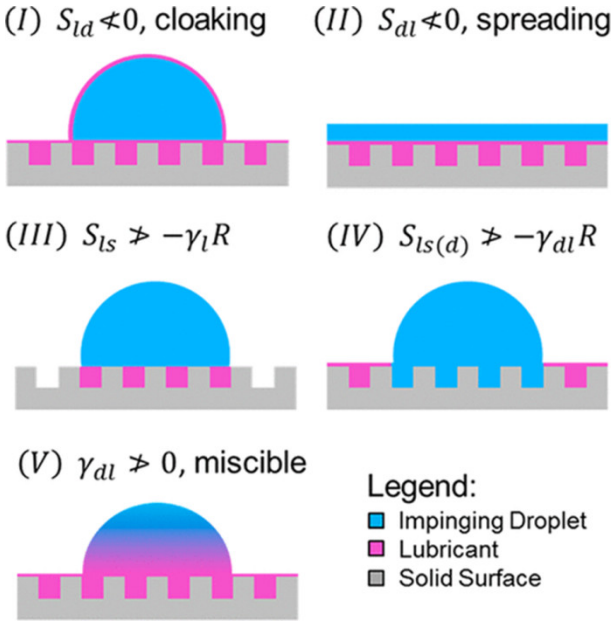

Figure 9. The possible failure modes outlined by Preston et al. for a lubricant/substrate/droplet system. The ideal droplet of impinging fluid on a slippery surface rests atop a combined lubricant-solid layer. Reproduced with permission from Ref. [221], Copyright 2017 American Chemical Society.

For slippery lubricating surfaces, when water droplets are frozen, the amount of lubricants greatly influences ice adhesion strength, accompanied by the depletion of lubricants during icing/de-icing cycles [223,224]. For example, Varanasi et al. demonstrated that ice adhesion strength of a lubricant-impregnated surface with excessive amount of lubricants was lower than that with balanced amount of lubricants by a factor of 15 (Figure 10a–c) [223]. Varanasi et al. also investigated the depletion phenomenon of lubricants before and after freezing and found that the impregnated lubricants can migrate from the wetting ridge and the substrate's texture to the frozen drop as observed by using the cryo-FIB/SEM images (Figure 10d–e) [224]. Once excessive amount of lubricants is depleted from substrate, inter-locking effect between ice and exposed hierarchical structures occurs, resulting in the increase of ice adhesion strength. Thus, this indicates that long-term use of SLIPS for surface icephobicity sometimes becomes impractical until the depletion problem of lubricants can be mitigated.

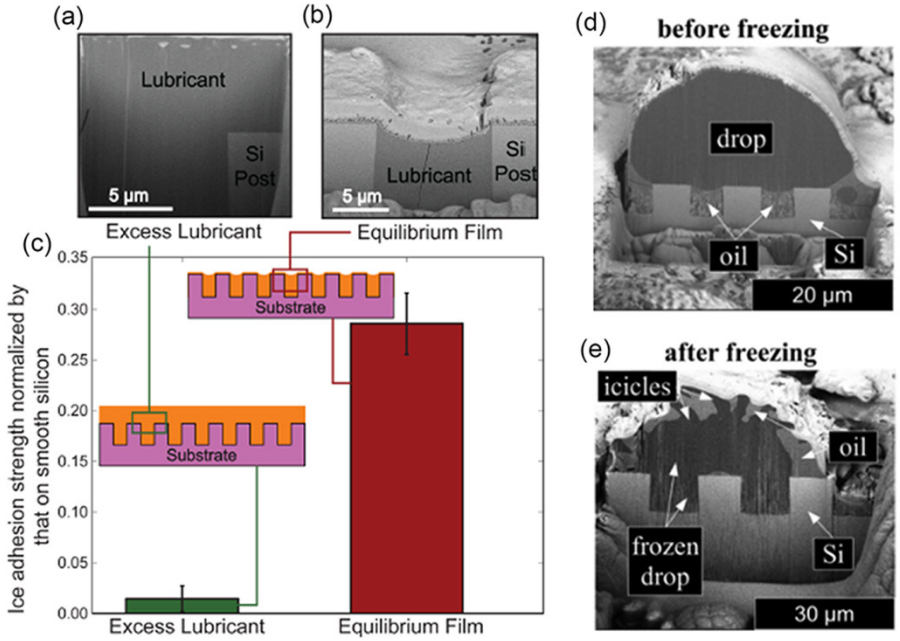

Figure 10. Cryo-stabilized SEM images of an FIB-cut lubricant-impregnated surface with (**a**) excess and (**b**) equilibrium films. (**c**) Comparison of the ice adhesion strength on lubricant-impregnated surfaces having excess and thermodynamically stable lubricant films. Cryo-FIB/SEM images of drops before (**d**) and after (**e**) freezing. The sample-holder assembly was cooled from room temperature to about −10 °C, and the relative humidity varied from 30 to 40%. (**a**–**c**) reproduced with permission from [223] and (**d**, **e**) reproduced with permission from [224], Copyright 2013 American Chemical Society.

To mitigate the depletion of lubricants, many efforts have been made to prepare durable SLIPS [24,35,68,73,74,90,132,225–227]. One strategy is to mix organic lubricants (e.g., oils) with polymer networks during synthesis; then, the added oils are released gradually under shear stress. For example, Golovin et al. fabricated a class of organic lubricants impregnated with durable elastomers with low ice adhesion strength [24]. Zhu et al. introduced a liquid-infused porous PDMS surface for icephobic coatings and achieved ice adhesion strength below 50 kPa (tensile test) and 40 kPa (shear test) [73]. Coady et al. developed an approach that utilized UV cross-linked, interpenetrated siloxane polymer networks to enhance SLIPS durability, obtaining ice adhesion strength below 10 kPa [68]. Yeong et al. reported a flexible oil-infused superhydrophobic elastomer with ice adhesion strength of ~38 kPa [90]. Pang et al. obtained waterborne anti-icing coatings with silicone oil microcapsules in latex paints for a long-term use [225]. Tao et al. prepared a durable slippery surface from polysiloxane and fluorinated POSS, which possessed an extremely low ice adhesion strength of 3.8 ± 1.8 kPa [226]. Gao et al. fabricated a durable, self-lubricating icephobic elastomer coating with ultra-low ice adhesion strength by optimizing silicone oil infusion levels [227]. Although the lubricants can be generated continuously during icing/de-icing cycles, the lubricant at the interface between ice and substrate is still easy to be depleted. To further improve the durability of SLIPS, new rational designs of organic lubricating layers have been proposed. Wang et al. used peanut oil as the lubricant that can have a phase transformation from liquid to solid state before water freezing and thus enhance the durability of obtained SLIPS [56].

In short, we discuss the design criteria and drawbacks of organic lubricating surfaces with icephobicity and summarize approaches towards improving the durability of organic lubricating surfaces during icing/de-icing cycles. Regarding lubricants, they need to be firmly locked by hierarchical (or porous) substrates and possess durable, regenerable, continuously released and/or phase transition properties during icing/de-icing cycles. For substrates, the anti-icing strategy of organic lubricating layers can be combined with other passive anti-icing strategies (e.g., low elastic and flexible substrates, sub-surface textured

substrates, etc.) to achieve synergistic effects and thus promote low ice adhesion strength. For organic lubricating layers, durability and longevity are still critical parameters that restrict practical applications. Considering the complexity of outdoor conditions and atmospheres, organic lubricating layers need to be properly chosen and utilized when used in the anti-icing field.

2.3.2. Aqueous Lubricating Surfaces

Compared with organic lubricating layers, aqueous lubricating layers for anti-icing application are due to a non-frozen liquid-like water layer that grafts hygroscopic molecules or polymers and then forms hydrophilic surfaces. This non-frozen liquid-like layer can exist at the ice-substrate interface below 0 °C and thus serves as a lubricating layer during a de-icing test [38,75,95,228–231]. Actually, the crucial question "Does the liquid-like layer exist at temperatures below 0 °C?" aroused researchers' curiosity for more than one century. As early as 1859, Michael Faraday hypothesized that a non-frozen liquid-like water layer covered ice even at temperatures well below freezing [229]. There are three interesting issues attracting researchers' attention: (1) temperatures that the non-frozen liquid layer begins to form; (2) the thickness of this non-frozen liquid layer; and (3) the reduction of ice adhesion strength caused by this non-frozen liquid layer.

With great effort, scientists have tried to found theories for the liquid-like non-frozen layer on ice. For example, in 1968 Fletcher developed a quantitative theory associated with the liquid-like water layer, and Fletcher's model predicts that the transition between the crystalline ice surface and the liquid-like water layer occurs at a well-defined temperature in the range from −6 to −3 °C [232]. Much experimental evidence, such as nuclear magnetic resonance (NMR), proton backscattering, X-ray diffraction and atomic force microscopy, shows that the liquid-like layer starts to form at a temperature range from −35 to 0 °C [229]. Dou et al. have experimentally verified the existence of the aqueous lubricating layer as low as −53 °C [36]. Besides, Xiao et al. demonstrated the presence of this liquid-like non-frozen layer by molecular dynamics simulation and showed a reduction of ice adhesion strength up to 60% [228]. Thus, the non-frozen liquid-like water layer may exist for the majority of de-icing tests on aqueous lubricating layers.

The thickness of the liquid-like layer can vary at different temperatures. For example, Döppenschmidt et al. used atomic force microscope (AFM) to investigate surface properties of ice in a temperature range from −24 to −0.7 °C and found the thickness of the liquid-like water layer varying between ~12 nm at −24 °C and ~70 nm at −0.7 °C [233]. Wettlaufer et al. reported that as temperature decreased, the slope of the film-thickness versus temperature curve changed depending on the relative strengths of van der Waals and Coulombic interactions because of the amount of impurity [234]. Ikeda-Fukazawa et al. performed molecular-dynamics studies of surface of ice Ih and found the thickness of liquid-like film as a function of temperature due to the surface melting of ice crystal and low friction [235]. Chen et al. found that for the hydrophobic surfaces, the interaction between water/ice and the substrate was dominated by van der Waal's forces [236], and the increased thickness of the water depletion layer at the interface weakened the van der Waal's interaction [75].

The investigation of non-frozen liquid-like lubricating layer for reducing ice adhesion strength becomes active in the recent decade. Usually, hydrophilic polymers can collect water in their vicinity as temperature decreases. For example, Chen et al. utilized several hydrophilic polymers to prepare aqueous lubricating layers with icephobicity, including hyaluronic acid-dopamine [38], poly(acrylic acid) (PAA) (Figure 11a) [76] and poly(acrylic acid)−dopamine [125], respectively. Dou et al. achieved ice adhesion strength of 27 ± 3 kPa at −15 °C on dimethylolpropionic acid/polyurethane surfaces [36]. Ozbay et al. used water, ethylene glycol, formamide and water-glycerine mixture as hydrophilic lubricants to prepare icephobic surfaces with a lowest ice adhesion strength of 16 ± 3 kPa [230]. Some researchers chose amphiphilic lubricants to replace traditional hydrophilic or hydrophobic lubricants to prepare lubricating surfaces, and potential synergistic effects

of hydrophilic and hydrophobic segments of amphiphilic lubricants showed high stability and excellent surface icephobicity [87,105,237,238]. Similarly, anti-freeze proteins [155,239], polyelectrolyte brush layers [77,240–244], hydrogels [139,245,246] and iongels [194] also contain hydrophilic and hydrophobic parts and can exhibit surface icephobicity. For example, Zhang et al., Yamazaki et al. and Wang et al. used anti-freeze hydrophilic liquids to obtain lubricating surfaces with excellent icephobicity at extremely low temperatures, including polyols [69], ethylene glycol [65] and ethanol (Figure 11b–d) [100]. Particularly, Wang et al. used the continuous release of ethanol molecules to generate the non-frozen liquid-like layer and realize low ice adhesion strength at low temperatures (Figure 11b–d) [100].

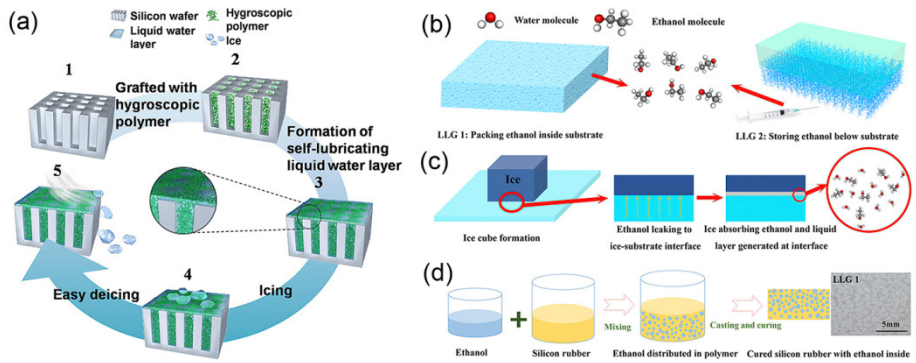

Figure 11. (**a**) Schematic illustration of the preparation of a self-lubricating liquid water layer surface: (**1**) Fabrication of microstructured silicon wafer. (**2**) Grafting hygroscopic polymers onto microstructured silicon wafer. (**3**) Self-lubricating liquid water layer forms on microstructured silicon wafer once the condensation occurs. (**4**) Ice formation atop of the self-lubricating liquid water layer. (**5**) Ice shed off with a wind action. Schematic illustration of the strategies of generating a liquid layer at the ice–substrate interface: (**b**) two strategies to create icephobic lubricating surfaces; (**c**) mechanism of generating a liquid ethanol layer at the ice–substrate interface; (**d**) fabricating method of lubricating surfaces: mixing ethanol with silicone rubber that can be quickly cured at room temperature, following which ethanol will be packed inside the substrate after curing. (**a**) Reproduced with permission from Ref. [76], Copyright 2013 American Chemical Society; (**b–d**) reproduced with permission from Ref. [100], Copyright 2019 The Royal Society of Chemistry.

In brief, aqueous lubricating layers show low ice adhesion strength because of the non-frozen liquid-like water layer below 0 °C. The non-frozen liquid-like layer forms from −53 to 0 °C, and the thickness of non-frozen liquid-like layer usually ranges from 0 to 100 nm, depending on temperatures and the impurity amount of water. Similar to other passive anti-icing strategies (e.g., organic lubricating layers, organogels), aqueous lubricating layers can realize super-low ice adhesion strength. The critical issue for aqueous lubricating layers is the sustainability of hygroscopic (or hydrophilic) polymers and thus the functional durability. Although much attention has been paid to the icing/de-icing cycles of aqueous lubricating layers, variations of chemical structures and morphologies of hygroscopic or hydrophilic polymers still need to be analyzed and explored after de-icing tests. Additionally, aqueous lubricating layers can be combined with other passive anti-icing strategies (i.e., elastic substrate and sub-surface structures) to achieve potential synergistic effects and thus facilitate lower ice adhesion strength. For the outdoor anti-icing application, however, the rational design of aqueous lubricating surfaces with durability and longevity at low temperature is still a challenge.

2.4. Sub-Surface Textured Surfaces

For textured surfaces, "Cassie ice" can be formed on hierarchical structures of SHSs, and micro-voids where trapped air exists become micro-cracks during a shear test. For example, Nosonovsky et al. explained why superhydrophobic surfaces were not always icephobic and concluded the correlation of ice adhesion strength with the receding contact

angle and the initial size of interfacial cracks [187]. Ling et al. reported that the formation of micro-cracks that act as interfacial stress concentrators can reduce ice adhesion strength on textured metallic surfaces [170]. Therefore, the key factor for textured surfaces with low ice adhesion strength is to form micro-cracks between ice and substrate and hence maximize interfacial cracking during a de-icing test.

According to the correlation between ice adhesion strength (τ_{ice} > 100 kPa) and (1 + cosθ_{rec}) proved by Meuler et al. [1] and He et al. [5], ice adhesion strength theoretically approaches zero when θ_{rec} becomes 180°. However, it is difficult to experimentally realize such a high receding contact angle. Thus, an alternative approach to obtaining low ice adhesion strength is proposed: hydrophobic surfaces (low surface energy) combining with sub-surface textured structures (potential crack initiators during the detachment of ice) (Figure 12a).

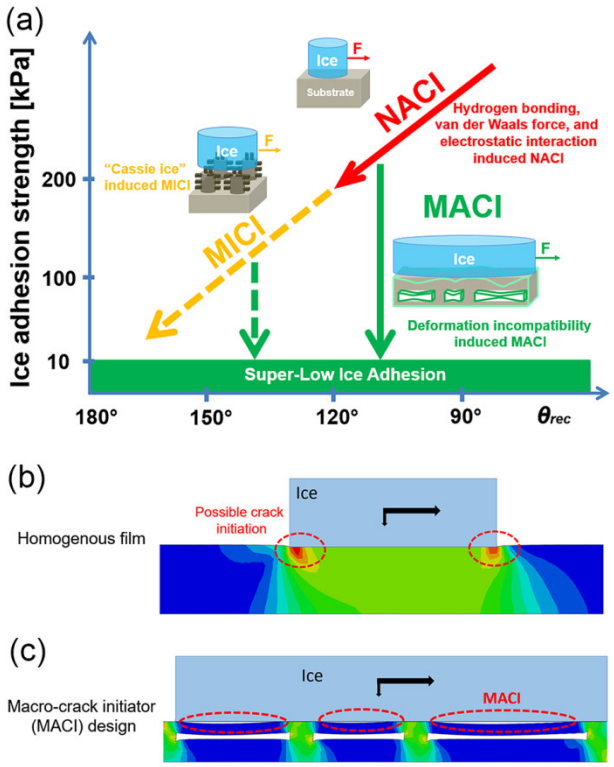

Figure 12. (**a**) Multiscale crack-initiator mechanisms at an ice–substrate interface. The red line represents nanoscale-initiator (NACI) mechanism. The yellow line denotes microscale-initiator (MICI) mechanism. The green lines show the proposed macroscale-initiator (MACI) mechanism that can function on any surfaces with deformation incompatibility, and bring ice adhesion strength down to the super-low regime. 2D plane strain finite element analyses using ABAQUS to illustrate the MACI mechanism, (**b**) ice adhesion test on a homogenous film and (**c**) ice adhesion test on the proposed film with substructures. The black arrows resemble the applied forces. (**a**–**d**) reproduced with permission from [13], Copyright 2017 the Royal Society of Chemistry.

From the viewpoint of fracture mechanics, it is hypothesized that multi-scale crack initiator-promoted surfaces with super-low ice adhesion strength can be obtained, and multi-scale crack initiators at the interface between ice and substrate can be divided into three types (Figure 12a): (1) nano-crack initiator (NACI) induced by the surface chemistry; (2) micro-crack initiator (MICI) formed by the micro-voids between the solid surface and the so-called "Cassie ice"; and (c) macro-crack initiator (MACI) induced by the stiffness inhomogeneity in both perpendicular and tangential directions (Figure 12b) to maximizing the length of crack (a) as suggested by the equation (1) during a shear test [13,140]. The experimental results confirmed that MACI originates from the deformation

incompatibility, which was fundamentally different from NACI and MICI as illustrated by finite element analyses (Figure 12b,c) [13].

Recently, multi-scale crack initiator-promoted surfaces with low ice adhesion strength have been developed by many researchers. For example, He et al. prepared sandwich-like PDMS sponges and realized durable super-low ice adhesion strength of 0.9 kPa by introducing MACI at the ice-substrate interface [2]. To understand the mechanism of MACI, He et al. investigated the effects of parameters on ice adhesion strength, including hollow sub-surface structure geometry (e.g., the heights, shapes, and distributions) and the directions of the applied shear force [140]. It is found that the number of potential crack initiation sites dictates the ice adhesion strength, and directions of the applied shear force can also influence the ice adhesion strength if the maximum length of an initiated crack is different [140]. Irajizad et al. developed interfacial crack-promoted icephobic surfaces with ice adhesion strength in order of 1 kPa and exceptional mechanical, chemical and environmental durability [143]. Chen et al. utilized a swelling force to induce the interfacial cracks and thus reduced ice adhesion strength of icephobic surfaces [247]. Chen et al. proposed a de-icing model that established a phase-change temperature gradient (ethanol solutions with different concentrations) at the interface to alter the contact stability between ice and substrate [248]. Jamil et al. obtained durable icephobic coatings by introducing Cassie–Baxter superhydrophobicity and cracks as caused by the incorporation of candle soot embedding and RTV-1 [146]. From the above discussion, the hypothesis on MACI promoted surfaces with super-low ice adhesion strength, providing new insight into the rational design of icephobic surfaces.

All in all, multi-scale crack initiator-promoted low ice adhesion surfaces (i.e., MACI) still need to be investigated both theoretically and experimentally, including the stability and durability of surfaces with sub-surface textured structures. Similarly, multi-scale crack initiator-promoted icephobic surfaces can be combined with other passive anti-icing strategies (i.e., aqueous/organic lubricating surfaces, SHSs and low elastic modulus surfaces) such that potential synergistic effects can help to overcome limitations of each individual anti-icing strategy and facilitate lowering ice adhesion strength.

3. Synergy of Multiple Anti-Icing Strategies

Individual passive anti-icing strategies have own drawbacks and ice adhesion strength on these strategies based icephobic surfaces may reach the theoretical limit. Thus, it is worth combining multiple passive anti-icing strategies to break the limitation of each individual strategy and further lower ice adhesion strength. For example, He et al. combined low elastic modulus substrate with aqueous lubricating layers [185] and multi-scale interfacial cracks [2,13,140] to achieve icephobic surfaces with low ice adhesion strength. Golovin et al. introduced organic lubricants into elastomers and obtained icephobic surfaces with extremely low ice adhesion strength [24,35]. Liu et al. integrated a superhydrophobic copper mesh with an intelligent organogel that can secrete anti-freezing agent (the mixture of ethylene glycol and water) autonomously in response to temperature, showing excellent icephobic properties [172]. Wang et al. prepared a robust anti-icing surface by combining low elastic modulus substrates with SHSs [206]. The synergistic effects of combining multiple passive anti-icing strategies can significantly reduce ice adhesion strength and offer a new solution to avoiding drawbacks and theoretical limits of passive anti-icing surfaces.

Currently, some researchers have introduced active anti-icing strategies (i.e., electro-thermal, photo-thermal and magnetic responsive stimulus) into passive icephobic surfaces to achieve the reliability and efficiency of de-icing, including magnetic-responsive icephobic surfaces [69,249,250], photo-thermal promoted icephobic surfaces [3,67,148,151,251–255] and electro-thermal icephobic surfaces (Figure 13) [104,151,256–258]. In this review, we focus on the rational design of passive anti-icing strategies by lowering ice adhesion strength, and the goal of the state-of-the-art icephobic surfaces is to realize ice adhesion strength as lowest as possible. In future, the combination of active and

passive anti-icing strategies is potentially a good choice for real outdoor anti-icing applications because such combined anti-icing strategy does not require achieving lowest ice adhesion strength but only needs to reach a certain value of ice adhesion strength and realize a rapid de-icing process with the assistance of active anti-icing strategies (i.e., magnetic-responsive, photo-thermal and electro-thermal stimulus). Thus, more relevant research needs to be investigated to study de-icing mechanisms and synergistic effects of active anti-icing strategies that promoted icephobic surfaces with low ice adhesion strength.

Figure 13. Multiple passive anti-icing combined strategies (i.e., smooth surfaces, textured surfaces, slippery surfaces and sub-surface textured surfaces) promoted by low ice adhesion surfaces. Active approaches (i.e., electro-thermal, photo-thermal and magnetic-responsive stimulus) can also be combined with passive anti-icing strategies for designing new icephobic surfaces in future.

4. Summary and Outlooks

Design and preparation of low ice adhesion surfaces for a long-term use is still a big challenge. Passive anti-icing strategies towards designing icephobic surfaces (i.e., smooth surfaces, textured surfaces, slippery surfaces and sub-surface textured surfaces) have their own advantages and disadvantages. For smooth surfaces, they usually need to be tuned by surface chemistry and elastic modulus to lower ice adhesion strength, which can incorporate with other anti-icing strategies (i.e., aqueous/organic lubricating layers and sub-surface structures) to reduce ice adhesion strength. For textured surfaces, the sustainability of surface chemistry and hierarchical structures becomes a critical issue to maintain surface icephobicity during icing/de-icing cycles. To enhance surface icephobicity, textured surfaces can introduce elastic/flexible substrates and/or hollow sub-surface structures (i.e., MACI) to lower ice adhesion strength. For slippery surfaces, low ice adhesion can be realized by rationally designing lubricating mechanisms and combining other passive anti-icing strategies (i.e., SHSs and sub-surface structures). For sub-surface textured surfaces (i.e., MACI), the combination of sub-surface textured surfaces with other passive anti-icing strategies becomes realistic, while the stability and longevity of the MACI strategy need to be investigated both theoretically and experimentally. Moreover, active anti-icing strategies (i.e., magnetic-responsive, photo-thermal and electro-thermal stimulus) can also be considered to combine with passive anti-icing strategies. In summary, each passive anti-icing strategy may have theoretical limits, and multiple passive (and/or active) anti-icing combined strategies promoted by low ice adhesion surfaces provide new insights and open an avenue towards designing novel icephobic surfaces in future.

Author Contributions: Conceptualization, Z.H., J.H. and Z.Z.; writing—original draft preparation, Z.H.; writing—review and editing, Z.H., Y.Z., J.H. and Z.Z. All authors have read and agreed to the published version of the manuscript.

Funding: This research was funded by the FRINATEK project Towards Design of Super-Low Ice Adhesion Surfaces (SLICE, 250990), the NANO2021 project Dual-Functional Anti-Gas Hydrate Surfaces (DAndra, 302348). Authors also thank the support of the Norwegian Micro- and Nano-Fabrication Facility (NorFab, 245963), the National Natural Science Foundation of China (Grant No. 51803043) and the Science Foundation of Hangzhou Dianzi University (KYS205620119)

Institutional Review Board Statement: Not applicable.

Informed Consent Statement: Not applicable.

Acknowledgments: We also thank Sigrid Rønneberg for her useful comments. Reproduced from Ref. [2], Ref. [13] and Ref. [100] with permission from the Royal Society of Chemistry.

Conflicts of Interest: The authors declare no conflict of interest.

References

1. Meuler, A.J.; Smith, J.D.; Varanasi, K.K.; Mabry, J.M.; McKinley, G.H.; Cohen, R.E. Relationships between water wettability and ice adhesion. *ACS Appl. Mater. Interfaces* **2010**, *2*, 3100–3110.
2. He, Z.; Zhuo, Y.; He, J.; Zhang, Z. Design and preparation of sandwich-like PDMS sponges with super-low ice adhesion. *Soft Matter* **2018**, *14*, 4846–4851.
3. Wu, S.W.; Du, Y.J.; Alsaid, Y.; Wu, D.; Hua, M.T.; Yan, Y.C.; Yao, B.W.; Ma, Y.F.; Zhu, X.Y.; He, X.M. Superhydrophobic photothermal icephobic surfaces based on candle soot. *Proc. Natl. Acad. Sci. USA* **2020**, *117*, 11240–11246.
4. Hejazi, V.; Sobolev, K.; Nosonovsky, M. From superhydrophobicity to icephobicity: Forces and interaction analysis. *Sci. Rep.* **2013**, *3*, 2194.
5. He, Z.; Vågenes, E.T.; Delabahan, C.; He, J.; Zhang, Z. Room temperature characteristics of polymer-based low ice adhesion surfaces. *Sci. Rep.* **2017**, *7*, 42181.
6. Liu, Y.H.; Moevius, L.; Xu, X.P.; Qian, T.Z.; Yeomans, J.M.; Wang, Z.K. Pancake bouncing on superhydrophobic surfaces. *Nat. Phys.* **2014**, *10*, 515–519.
7. Deng, X.; Mammen, L.; Butt, H.-J.; Vollmer, D. Candle soot as a template for a transparent robust superamphiphobic coating. *Science* **2012**, *335*, 67–70.
8. Genzer, J.; Efimenko, K. Creating long-lived superhydrophobic polymer surfaces through mechanically assembled monolayers. *Science* **2000**, *290*, 2130–2133.
9. Wen, M.; Wang, L.; Zhang, M.; Jiang, L.; Zheng, Y. Antifogging and icing-delay properties of composite micro- and nanostructured surfaces. *ACS Appl. Mater. Interfaces* **2014**, *6*, 3963–3968.
10. Boreyko, J.B.; Collier, C.P. Delayed frost growth on jumping-drop superhydrophobic surfaces. *ACS Nano* **2013**, *7*, 1618–1627.
11. Guo, P.; Zheng, Y.; Wen, M.; Song, C.; Lin, Y.; Jiang, L. Icephobic/anti-icing properties of micro/nanostructured surfaces. *Adv. Mater.* **2012**, *24*, 2642–2648.
12. Varanasi, K.K.; Deng, T.; Smith, J.D.; Hsu, M.; Bhate, N. Frost formation and ice adhesion on superhydrophobic surfaces. *Appl. Phys. Lett.* **2010**, *97*, 234102–234103.
13. He, Z.; Xiao, S.; Gao, H.; He, J.; Zhang, Z. Multiscale crack initiator promoted super-low ice adhesion surfaces. *Soft Matter* **2017**, *13*, 6562–6568.
14. Lv, J.; Song, Y.; Jiang, L.; Wang, J. Bio-inspired strategies for anti-icing. *ACS Nano* **2014**, *8*, 3152–3169.
15. Zhang, S.; Huang, J.; Cheng, Y.; Yang, H.; Chen, Z.; Lai, Y. Bioinspired Surfaces with Superwettability for Anti-Icing and Ice-Phobic Application: Concept, Mechanism, and Design. *Small* **2017**, *13*, 1701867.
16. Sojoudi, H.; Wang, M.; Boscher, N.D.; McKinley, G.H.; Gleason, K.K. Durable and scalable icephobic surfaces: Similarities and distinctions from superhydrophobic surfaces. *Soft Matter* **2016**, *12*, 1938–1963.
17. Wang, F.; Zhuo, Y.; He, Z.; Xiao, S.; He, J.; Zhang, Z. Dynamic Anti-Icing Surfaces (DAIS). *Adv. Sci.* **2021**, 2101163, https://doi.org/10.1002/advs.202101163.
18. Zhuo, Y.; Xiao, S.; Amirfazli, A.; He, J.; Zhang, Z. Polysiloxane as icephobic Materials—The past, present and the future. *Chem. Eng. J.* **2020**, *405*, 127088.
19. Zhuo, Y.; Chen, J.; Xiao, S.; Li, T.; Wang, F.; He, J.; Zhang, Z. Gels as emerging anti-icing materials: A mini review. *Mater. Horizons* **2021,** DOI: 10.1039/D1MH00910A.
20. Esmeryan, K.D. From extremely water-repellent coatings to passive icing protection—principles, limitations and lnnovative application aspects. *Coatings* **2020**, *10*, 66.
21. He, Z.; Shen, Z.; Qiu, H.; Chen, J.; Liang, L.; Wang, J. Research progress in aluminium-based anti-icing surfaces. *J. Mater. Eng.* **2021**, *49*, 41–50.
22. Wang, G.; Guo, Z. Liquid infused surfaces with anti-icing properties. *Nanoscale* **2019**, *11*, 22615–22635.

23. Latthe, S.S.; Sutar, R.S.; Bhosale, A.K.; Nagappan, S.; Ha, C.-S.; Sadasivuni, K.K.; Liu, S.; Xing, R. Recent developments in air-trapped superhydrophobic and liquid-infused slippery surfaces for anti-icing application. *Prog. Org. Coat.* **2019**, *137*, 105373.
24. Golovin, K.; Kobaku, S.P.; Lee, D.H.; DiLoreto, E.T.; Mabry, J.M.; Tuteja, A. Designing durable icephobic surfaces. *Sci. Adv.* **2016**, *2*, e1501496.
25. Rønneberg, S.; He, J.; Zhang, Z. The need for standards in low ice adhesion surface research: A critical review. *J. Adhes. Sci. Technol.* **2019**, *34*, 1–29.
26. Rønneberg, S.; Laforte, C.; Volat, C.; He, J.; Zhang, Z. The effect of ice type on ice adhesion. *AIP Adv.* **2019**, *9*, 055304.
27. Brassard, J.-D.; Laforte, C.; Guérin, F.; Blackburn, C. Icephobicity: Definition and measurement regarding atmospheric icing. *Adv. Polym. Sci.* **2017**, *284*, 123-143.
28. Golovin, K.; Dhyani, A.; Thouless, M.D.; Tuteja, A. Low–interfacial toughness materials for effective large-scale deicing. *Science* **2019**, *364*, 371–375.
29. Makkonen, L. Ice adhesion —Theory, measurements and countermeasures. *J. Adhes. Sci. Technol.* **2012**, *26*, 413–445.
30. Andrews, E.H.; Majid, H.A.; Lockington, N.A. Adhesion of ice to a flexible substrate. *J. Mater Sci* **1984**, *19*, 73–81.
31. Liu, B.; Zhang, K.; Tao, C.; Zhao, Y.; Li, X.; Zhu, K.; Yuan, X. Strategies for anti-icing: Low surface energy or liquid-infused? *RSC Adv.* **2016**, *6*, 70251–70260.
32. Fu, Q.; Wu, X.; Kumar, D.; Ho, J.W.C.; Kanhere, P.D.; Srikanth, N.; Liu, E.; Wilson, P.; Chen, Z. Development of sol–gel icephobic coatings: Effect of surface roughness and surface energy. *ACS Appl. Mater. Interfaces* **2014**, *6*, 20685–20692.
33. Foroughi Mobarakeh, L.; Jafari, R.; Farzaneh, M. Robust icephobic, and anticorrosive plasma polymer coating. *Cold Reg. Sci. Technol.* **2018**, *151*, 89–93.
34. Foroughi Mobarakeh, L.; Jafari, R.; Farzaneh, M. The ice repellency of plasma polymerized hexamethyldisiloxane coating. *Appl. Surf. Sci.* **2013**, *284*, 459–463.
35. Golovin, K.; Tuteja, A. A predictive framework for the design and fabrication of icephobic polymers. *Sci. Adv.* **2017**, *3*, e1701617.
36. Dou, R.; Chen, J.; Zhang, Y.; Wang, X.; Cui, D.; Song, Y.; Jiang, L.; Wang, J. Anti-icing coating with an aqueous lubricating layer. *ACS Appl. Mater. Interfaces* **2014**, *6*, 6998–7003.
37. Cui, W.; Pakkanen, T.A. Fabrication of transparent icephobic surfaces with self-reparability: Effect of structuring and thickness of the lubricant-elastomer layer. *Appl. Surf. Sci.* **2019**, *504*, 144061.
38. Chen, J.; Luo, Z.; Fan, Q.; Lv, J.; Wang, J. Anti-ice coating inspired by ice skating. *Small* **2014**, *10*, 4693–4699.
39. Chen, J.; Liu, J.; He, M.; Li, K.; Cui, D.; Zhang, Q.; Zeng, X.; Zhang, Y.; Wang, J.; Song, Y. Superhydrophobic surfaces cannot reduce ice adhesion. *Appl. Phys. Lett.* **2012**, *101*, 111603.
40. Balordi, M.; Santucci de Magistris, G.; Chemelli, C. A novel simple anti-ice aluminum coating: Synthesis and in-lab comparison with a superhydrophobic hierarchical surface. *Coatings* **2020**, *10*, 111.
41. Beemer, D.L.; Wang, W.; Kota, A.K. Durable gels with ultra-low adhesion to ice. *J. Mater. Chem. A* **2016**, *4*, 18253–18258.
42. Chen, G.; Liu, S.; Sun, Z.; Wen, S.; Feng, T.; Yue, Z. Intrinsic self-healing organogels based on dynamic polymer network with self-regulated secretion of liquid for anti-icing. *Prog. Org. Coat.* **2020**, *144*, 105641.
43. Barman, T.; Chen, H.; Liu, J.; Yang, G.; Zhao, W.; Peng, C.; Hou, X. Synthesis and characterization of styrene-based polyfluoro-acrylate film for hydrophobic/icephobic applications. *Thin Solid Films* **2019**, *687*, 137462.
44. Barthwal, S.; Lee, B.; Lim, S.-H. Fabrication of robust and durable slippery anti-icing coating on textured superhydrophobic aluminum surfaces with infused silicone oil. *Appl. Surf. Sci.* **2019**, *496*, 143677.
45. Aguilar, D.; Zheng, S.; Huang, Y.; Zeng, X.; Zhang, Q.; Chen, Z. Solvent-free synthesis and hydrophobization of bio-based epoxy coatings for anti-icing and anticorrosion applications. *ACS Sustain. Chem. Eng.* **2019**, *7*, 19131–19141.
46. Arianpour, F.; Farzaneh, M.; Kulinich, S.A. Hydrophobic and ice-retarding properties of doped silicone rubber coatings. *Appl. Surf. Sci.* **2013**, *265*, 546–552.
47. Saleema, N.; Farzaneh, M.; Paynter, R.W.; Sarkar, D.K. Prevention of ice accretion on aluminum surfaces by enhancing their hydrophobic properties. *J. Adhes. Sci. Technol.* **2011**, *25*, 27–40.
48. Arianpour, F.; Farzaneh, M.; Jafari, R. Hydrophobic and ice-phobic properties of self-assembled monolayers (SAMs) coatings on AA*Prog. Org. Coat.* **2016**, *93*, 41–45.
49. Shen, Y.; Tao, H.; Chen, S.; Zhu, L.; Wang, T.; Tao, J. Icephobic/anti-icing potential of superhydrophobic Ti_6Al_4V surfaces with hierarchical textures. *RSC Adv.* **2015**, *5*, 1666–1672.
50. Susoff, M.; Siegmann, K.; Pfaffenroth, C.; Hirayama, M. Evaluation of icephobic coatings—Screening of different coatings and influence of roughness. *Appl. Surf. Sci.* **2013**, *282*, 870–879.
51. Tang, L.; Wang, N.; Han, Z.; Sun, H.; Xiong, D. Robust superhydrophobic surface with wrinkle-like structures on AZ31 alloy that repels viscous oil and investigations of the anti-icing property. *Colloid Surface. A* **2020**, *594*, 124655.
52. Valentini, L.; Bittolo Bon, S.; Pugno, N.M.; Hernandez Santana, M.; Lopez-Manchado, M.A.; Giorgi, G. Synergistic icephobic behaviour of swollen nitrile butadiene rubber graphene and/or carbon nanotube composites. *Compos. Part B-Eng.* **2019**, *166*, 352–360.
53. Wang, C.; Fuller, T.; Zhang, W.; Wynne, K.J. Thickness dependence of ice removal stress for a polydimethylsiloxane nanocomposite: Sylgard. *Langmuir* **2014**, *30*, 12819–12826.
54. Wang, C.; Gupta, M.C.; Yeong, Y.H.; Wynne, K.J. Factors affecting the adhesion of ice to polymer substrates. *J. Appl. Polym. Sci.* **2017**, *135*, 45734.

55. Wang, C.; Zhang, W.; Siva, A.; Tiea, D.; Wynne, K.J. Laboratory test for ice adhesion strength using commercial instrumentation. *Langmuir* **2014**, *30*, 540–547.
56. Wang, F.; Ding, W.; He, J.; Zhang, Z. Phase transition enabled durable anti-icing surfaces and its DIY design. *Chem. Eng. J.* **2019**, *360*, 243–249.
57. Wang, G.; Shen, Y.; Tao, J.; Luo, X.; Zhang, L.; Xia, Y. Fabrication of a superhydrophobic surface with a hierarchical nanoflake-micropit structure and its anti-icing properties. *RSC Adv.* **2017**, *7*, 9981–9988.
58. Wang, J.; Memon, H.; Liu, J.; Yang, G.; Xu, F.; Hussain, T.; Scotchford, C.; Hou, X. Effect of surface adsorption on icing behaviour of metallic coating. *Surf. Coat. Technol.* **2019**, *380*, 125068.
59. Wang, Y.; Liu, J.; Li, M.; Wang, Q.; Chen, Q. The icephobicity comparison of polysiloxane modified hydrophobic and superhydrophobic surfaces under condensing environments. *Appl. Surf. Sci.* **2016**, *385*, 472–480.
60. Wang, Y.; Xue, J.; Wang, Q.; Chen, Q.; Ding, J. Verification of icephobic/anti-icing properties of a superhydrophobic surface. *ACS Appl. Mater. Interfaces* **2013**, *5*, 3370–3381.
61. Wu, X.; Chen, Z. A mechanically robust transparent coating for anti-icing and self-cleaning applications. *J. Mater. Chem. A* **2018**, *6*, 16043–16052.
62. Wu, X.; Silberschmidt, V.V.; Hu, Z.-T.; Chen, Z. When superhydrophobic coatings are icephobic: Role of surface topology. *Surf. Coat. Technol.* **2019**, *358*, 207–214.
63. Wu, X.H.; Tang, Y.X.; Silberschmidt, V.V.; Wilson, P.; Chen, Z. Mechanically robust transparent anti-icing coatings: Roles of dispersion status of titanate nanotubes. *Adv. Mater. Interfaces* **2018**, *5*, 1800773.
64. Wu, X.H.; Zheng, S.L.; Bellido-Aguilar, D.A.; Silberschmidt, V.V.; Chen, Z. Transparent icephobic coatings using bio-based epoxy resin. *Mater. Des.* **2018**, *140*, 516–523.
65. Yamazaki, T.; Tenjimbayashi, M.; Manabe, K.; Moriya, T.; Nakamura, H.; Nakamura, T.; Matsubayashi, T.; Tsuge, Y.; Shiratori, S. Antifreeze liquid-Infused surface with high transparency, low ice adhesion strength, and antifrosting properties fabricated through a spray layer-by-layer method. *Ind. Eng. Chem. Res.* **2019**, *58*, 2225–2234.
66. Yang, Q.; Zhu, Z.; Tan, S.; Luo, Y.; Luo, Z. How micro-/nano-structure evolution influences dynamic wetting and natural deicing abilities of bionic lotus surfaces. *Langmuir* **2020**, *36*, 4005–4014.
67. Yin, X.; Zhang, Y.; Wang, D.; Liu, Z.; Liu, Y.; Pei, X.; Yu, B.; Zhou, F. Integration of self-lubrication and near-infrared photothermogenesis for excellent anti-icing/deicing performance. *Adv. Funct. Mater.* **2015**, *25*, 4237–4245.
68. Coady, M.J.; Wood, M.; Wallace, G.Q.; Nielsen, K.E.; Kietzig, A.-M.; Lagugné-Labarthet, F.; Ragogna, P.J. Icephobic behavior of UV-cured polymer networks incorporated into slippery lubricant-infused porous surfaces: Improving SLIPS durability. *ACS Appl. Mater. Interfaces* **2018**, *10*, 2890–2896.
69. Zhang, G.; Zhang, Q.; Cheng, T.; Zhan, X.; Chen, F. Polyols-infused slippery surfaces based on magnetic Fe_3O_4-functionalized polymer hybrids for enhanced multifunctional anti-icing and deicing properties. *Langmuir* **2018**, *34*, 4052–4058.
70. Zhang, J.; Gu, C.; Tu, J. Robust slippery coating with superior corrosion resistance and anti-icing performance for AZ31B Mg alloy protection. *ACS Appl. Mater. Interfaces* **2017**, *9*, 11247–11257.
71. Zhang, J.; Liu, B.; Tian, Y.; Wang, F.; Chen, Q.; Zhang, F.; Qian, H.; Ma, L. Facile one-step method to fabricate a slippery lubricant-infused surface (LIS) with self-replenishment properties for anti-icing applications. *Coatings* **2020**, *10*, 119.
72. Zhu, K.; Li, X.; Su, J.; Li, H.; Zhao, Y.; Yuan, X. Improvement of anti-icing properties of low surface energy coatings by introducing phase-change microcapsules. *Polym. Eng. Sci.* **2018**, *58*, 973–979.
73. Zhu, L.; Xue, J.; Wang, Y.; Chen, Q.; Ding, J.; Wang, Q. Ice-phobic coatings based on silicon-oil-infused polydimethylsiloxane. *ACS Appl. Mater. Interfaces* **2013**, *5*, 4053–4062.
74. Zhuo, Y.; Wang, F.; Xiao, S.; He, J.; Zhang, Z. One-step fabrication of bioinspired lubricant-regenerable icephobic slippery liquid-infused porous surfaces. *ACS Omega* **2018**, *3*, 10139–10144.
75. Chen, D.; Gelenter, M.D.; Hong, M.; Cohen, R.E.; McKinley, G.H. Icephobic surfaces induced by interfacial nonfrozen water. *ACS Appl. Mater. Interfaces* **2017**, *9*, 4202–4214.
76. Chen, J.; Dou, R.; Cui, D.; Zhang, Q.; Zhang, Y.; Xu, F.; Zhou, X.; Wang, J.; Song, Y.; Jiang, L. Robust prototypical anti-icing coatings with a self-lubricating liquid water layer between ice and substrate. *ACS Appl. Mater. Interfaces* **2013**, *5*, 4026–4030.
77. Chernyy, S.; Järn, M.; Shimizu, K.; Swerin, A.; Pedersen, S.U.; Daasbjerg, K.; Makkonen, L.; Claesson, P.; Iruthayaraj, J. Superhydrophilic polyelectrolyte brush layers with imparted anti-icing properties: Effect of counter ions. *ACS Appl. Mater. Interfaces* **2014**, *6*, 6487–6496.
78. Zhuo, Y.; Xiao, S.; Håkonsen, V.; Li, T.; Wang, F.; He, J.; Zhang, Z. Ultrafast self-healing and highly transparent coating with mechanically durable icephobicity. *Appl. Mater. Today* **2020**, *19*, 100542.
79. Zou, M.; Beckford, S.; Wei, R.; Ellis, C.; Hatton, G.; Miller, M.A. Effects of surface roughness and energy on ice adhesion strength. *Appl. Surf. Sci.* **2011**, *257*, 3786–3792.
80. Zheng, S.; Li, C.; Fu, Q.; Xiang, T.; Hu, W.; Wang, J.; Ding, S.; Liu, P.; Chen, Z. Fabrication of a micro-nanostructured superhydrophobic aluminum surface with excellent corrosion resistance and anti-icing performance. *RSC Adv.* **2016**, *6*, 79389–79400.
81. Zhuo, Y.; Li, T.; Wang, F.; Håkonsen, V.; Xiao, S.; He, J.; Zhang, Z. Ultra-durable icephobic coating by molecular pulley. *Soft Matter* **2019**, *15*, 3607–3611.
82. Zheng, S.; Li, C.; Fu, Q.; Hu, W.; Xiang, T.; Wang, Q.; Du, M.; Liu, X.; Chen, Z. Development of stable superhydrophobic coatings on aluminum surface for corrosion-resistant, self-cleaning, and anti-icing applications. *Mater. Des.* **2016**, *93*, 261–270.

83. Zheng, S.; Bellido-Aguilar, D.A.; Wu, X.; Zhan, X.; Huang, Y.; Zeng, X.; Zhang, Q.; Chen, Z. Durable waterborne hydrophobic bio-epoxy coating with improved anti-icing and self-cleaning performance. *ACS Sustain. Chem. Eng.* **2018**, *7*, 641–649.
84. Zhang, L.; Guo, Z.; Sarma, J.; Dai, X. Passive removal of highly wetting liquids and ice on quasi-liquid surfaces. *ACS Appl. Mater. Interfaces* **2020**, *12*, 20084–20095.
85. Zhang, K.-q.; Cai, J.-z.; Li, X.-h.; Li, H.; Zhao, Y.-h.; Yuan, X.-y. Balance of polyacrylate-fluorosilicone block copolymers as icephobic coatings. *Chin. J. Polym. Sci.* **2015**, *33*, 153–162.
86. Zhang, K.; Li, X.; Zhao, Y.; Zhu, K.; Li, Y.; Tao, C.; Yuan, X. UV-curable POSS-fluorinated methacrylate diblock copolymers for icephobic coatings. *Prog. Org. Coat.* **2016**, *93*, 87–96.
87. Yu, Y.; Jin, B.; Jamil, M.I.; Cheng, D.-G.; Zhang, Q.; Zhan, X.; Chen, F. Highly stable amphiphilic organogel with exceptional anti-icing performance. *ACS Appl. Mater. Interfaces* **2019**, *11*, 12838–12845.
88. Yu, D.; Zhao, Y.; Li, H.; Qi, H.; Li, B.; Yuan, X. Preparation and evaluation of hydrophobic surfaces of polyacrylate-polydimethylsiloxane copolymers for anti-icing. *Prog. Org. Coat.* **2013**, *76*, 1435–1444.
89. Yin, Y.; Liu, M.H.; Wei, W.; Zhang, Y.F.; Gutowski, V.; Zhang, W.X.; Deng, P.Y. "Open-mouth" mesoporous hollow micro/nano coatings based on POSS/PDMS: Fabrication, mechanisms, and anti-icing performance. *Part. Part. Syst. Char.* **2018**, *35*, 1800323.
90. Yeong, Y.H.; Wang, C.; Wynne, K.J.; Gupta, M.C. Oil-infused superhydrophobic silicone material for low ice adhesion with long-term infusion stability. *ACS Appl. Mater. Interfaces* **2016**, *8*, 32050–32059.
91. Yeong, Y.H.; Gupta, M.C. Hot embossed micro-textured thin superhydrophobic Teflon FEP sheets for low ice adhesion. *Surf. Coat. Technol.* **2017**, *313*, 17–23.
92. Wu, X.H.; Zhao, X.; Ho, J.W.C.; Chen, Z. Design and durability study of environmental-friendly room-temperature processable icephobic coatings. *Chem. Eng. J.* **2019**, *355*, 901–909.
93. Wu, Y.-l.; She, W.; Shi, D.; Jiang, T.; Hao, T.-h.; Liu, J.; Zhang, Q.-c.; You, J.; Li, R.Y. An extremely chemical and mechanically durable siloxane bearing copolymer coating with self-crosslinkable and anti-icing properties. *Compos. Part B-Eng.* **2020**, *195*, 108031.
94. Xu, Y.; Zhang, G.; Li, L.; Xu, C.; Lv, X.; Zhang, H.; Yao, W. Icephobic behaviors of superhydrophobic amorphous carbon nanofilms synthesized from a flame process. *J. Colloid Interface Sci.* **2019**, *552*, 613–621.
95. Wen, S.F.; Wang, Y.M.; Zhang, Z.M.; Liu, Y.L. Application of anti-icing coating based on adsorption of functional substances by microporous sphere. *Prog. Org. Coat.* **2019**, *137*, 105320.
96. Wei, C.; Jin, B.; Zhang, Q.; Zhan, X.; Chen, F. Anti-icing performance of super-wetting surfaces from icing-resistance to icephobic aspects: Robust hydrophobic or slippery surfaces. *J. Alloy Compd.* **2018**, *765*, 721–730.
97. Wang, Y.; Yao, X.; Chen, J.; He, Z.; Liu, J.; Li, Q.; Wang, J.; Jiang, L. Organogel as durable anti-icing coatings. *Sci. China Mater.* **2015**, *58*, 559–565.
98. Wang, Y.; Li, M.; Lv, T.; Wang, Q.; Chen, Q.; Ding, J. Influence of different chemical modifications on the icephobic properties of superhydrophobic surfaces in a condensate environment. *J. Mater. Chem. A* **2015**, *3*, 4967–4975.
99. Wang, N.; Tang, L.L.; Tong, W.; Xiong, D.S. Fabrication of robust and scalable superhydrophobic surfaces and investigation of their anti-icing properties. *Mater. Des.* **2018**, *156*, 320–328.
100. Wang, F.; Xiao, S.; Zhuo, Y.; Ding, W.; He, J.; Zhang, Z. Liquid layer generators for excellent icephobicity at extremely low temperatures. *Mater. Horizons* **2019**, *6*, 2063–2072.
101. Wang, F.; Tay, T.E.; Sun, Y.; Liang, W.; Yang, B. Low-voltage and -surface energy SWCNT/poly(dimethylsiloxane) (PDMS) nanocomposite film: Surface wettability for passive anti-icing and surface-skin heating for active deicing. *Compos. Sci. Technol.* **2019**, *184*, 107872.
102. Vercillo, V.; Tonnicchia, S.; Romano, J.M.; Garcia-Giron, A.; Aguilar-Morales, A.I.; Alamri, S.; Dimov, S.S.; Kunze, T.; Lasagni, A.F.; Bonaccurso, E. Design rules for laser-treated icephobic metallic surfaces for aeronautic applications. *Adv. Funct. Mater.* **2020**, *30*, 1910268.
103. Vazirinasab, E.; Maghsoudi, K.; Jafari, R.; Momen, G. A comparative study of the icephobic and self-cleaning properties of teflon materials having different surface morphologies. *J. Mater. Process. Tech.* **2019**, *276*, 116415.
104. Urata, C.; Hönes, R.; Sato, T.; Kakiuchida, H.; Matsuo, Y.; Hozumi, A. Textured organogel films showing unusual thermoresponsive dewetting, icephobic, and optical properties. *Adv. Mater. Interfaces* **2019**, *6*, 1801358.
105. Upadhyay, V.; Galhenage, T.; Battocchi, D.; Webster, D. Amphiphilic icephobic coatings. *Prog. Org. Coat.* **2017**, *112*, 191–199.
106. Taş, M.; Memon, H.; Xu, F.; Ahmed, I.; Hou, X. Electrospun nanofibre membrane based transparent slippery liquid-infused porous surfaces with icephobic properties. *Colloid Surface. A* **2019**, *585*, 124177.
107. Tarquini, S.; Antonini, C.; Amirfazli, A.; Marengo, M.; Palacios, J. Investigation of ice shedding properties of superhydrophobic coatings on helicopter blades. *Cold Reg. Sci. Technol.* **2014**, *100*, 50–58.
108. Sojoudi, H.; McKinley, G.H.; Gleason, K.K. Linker-free grafting of fluorinated polymeric cross-linked network bilayers for durable reduction of ice adhesion. *Mater. Horizons* **2015**, *2*, 91–99.
109. Sojoudi, H.; Arabnejad, H.; Raiyan, A.; Shirazi, S.A.; McKinley, G.H.; Gleason, K.K. Scalable and durable polymeric icephobic and hydrate-phobic coatings. *Soft Matter* **2018**, *14*, 3443–3454.
110. Sivakumar, G.; Jackson, J.; Ceylan, H.; Sundararajan, S. Effect of plasticizer on the wear behavior and ice adhesion of elastomeric coatings. *Wear* **2019**, *426-427*, 212-218.
111. Shen, Y.; Wu, Y.; Tao, J.; Zhu, C.; Chen, H.; Wu, Z.; Xie, Y. Spraying fabrication of durable and transparent coatings for anti-icing application: Dynamic water repellency, icing delay, and ice adhesion. *ACS Appl. Mater. Interfaces* **2019**, *11*, 3590–3598.

112. Shen, Y.; Tao, J.; Tao, H.; Chen, S.; Pan, L.; Wang, T. Superhydrophobic Ti_6Al_4V surfaces with regular array patterns for anti-icing applications. *RSC Adv.* **2015**, *5*, 32813–32818.
113. Sandhu, A.; Walker, O.J.; Nistal, A.; Choy, K.L.; Clancy, A.J. Perfluoroalkane wax infused gels for effective, regenerating, anti-icing surfaces. *Chem. Commun.* **2019**, *55*, 3215–3218.
114. Qin, C.; Mulroney, A.T.; Gupta, M.C. Anti-icing epoxy resin surface modified by spray coating of PTFE teflon particles for wind turbine blades. *Mater. Today Commun.* **2019**, *22*, 100770.
115. Nguyen, T.-B.; Park, S.; Lim, H. Effects of morphology parameters on anti-icing performance in superhydrophobic surfaces. *Appl. Surf. Sci.* **2018**, *435*, 585–591.
116. Nguyen, T.-B.; Park, S.; Jung, Y.; Lim, H. Effects of hydrophobicity and lubricant characteristics on anti-icing performance of slippery lubricant-infused porous surfaces. *J. Ind. Eng. Chem.* **2018**, *69*, 99–105.
117. Mulroney, A.T.; Kessler, E.D.; Combs, S.; Gupta, M.C. Low ice adhesion surfaces using microtextured hydrophobic tapes and their applications in refrigeration systems. *Surf. Coat. Technol.* **2018**, *351*, 108–114.
118. Ahn, J.; Jeon, J.; Heu, C.S.; Kim, D.R. Three-dimensionally programmed slippery wrinkles with high stretchability for tunable functionality of icephobicity and effective water harvesting. *Adv. Mater. Interfaces* **2018**, *5*, 1800980.
119. Arianpour, F.; Farhadi, S.; Farzaneh, M. Effect of heterogeneity on hydro/ice-phobic properties of alkylsilane/fluoro-alkylsilane-based coatings on Al substrates. *J. Coat. Technol. Res.* **2017**, *14*, 267–275.
120. Balordi, M.; Cammi, A.; de Magistris, G.S.; Chemelli, C. Role of micrometric roughness on anti-ice properties and durability of hierarchical super-hydrophobic aluminum surfaces. *Surf. Coat. Technol.* **2019**, *374*, 549–556.
121. Bleszynski, M.; Woll, R.; Middleton, J.; Kumosa, M. Effects of crosslinking, embedded TiO_2 particles and extreme aging on PDMS icephobic barriers. *Polym. Degrad. Stabil.* **2019**, *166*, 272–282.
122. Boinovich, L.B.; Zhevnenko, S.N.; Emel'yanenko, A.M.; Gol'dshtein, R.V.; Epifanov, V.P. Adhesive strength of the contact of ice with a superhydrophobic coating. *Dokl. Chem.* **2013**, *448*, 71–75.
123. Momen, G.; Jafari, R.; Farzaneh, M. Ice repellency behaviour of superhydrophobic surfaces: Effects of atmospheric icing conditions and surface roughness. *Appl. Surf. Sci.* **2015**, *349*, 211–218.
124. Brassard, J.-D.; Laforte, J.-L.; Blackburn, C.; Perron, J.; Sarkar, D.K. Silicone based superhydrophobic coating efficient to reduce ice adhesion and accumulation on aluminum under offshore arctic conditions. *Ocean Eng.* **2017**, *144*, 135–141.
125. Chen, J.; Li, K.; Wu, S.; Liu, J.; Liu, K.; Fan, Q. Durable anti-icing coatings based on self-sustainable lubricating layer. *ACS Omega* **2017**, *2*, 2047–2054.
126. Chu, Z.M.; Jiao, W.C.; Huang, Y.F.; Ding, G.M.; Zhong, X.; Yan, M.L.; Zheng, Y.T.; Wang, R.G. FDTS-modified SiO_2/rGO wrinkled films with a micro-nanoscale hierarchical structure and anti-icing/deicing properties under condensation condition. *Adv. Mater. Interfaces* **2020**, *7*, 1901446.
127. Coady, M.J.; Getangama, N.N.K.; Khalili, A.; Wood, M.; Nielsen, K.E.; de Bruyn, J.R.; Hutter, J.L.; Klassen, R.J.; Kietzig, A.M.; Ragogna, P.J. Highly cross-linked UV-cured siloxane copolymer networks as icephobic coatings. *J. Polym. Sci.* **2020**, *58*, 1022–1029.
128. Cui, W.; Jiang, Y.; Mielonen, K.; Pakkanen, T.A. The verification of icephobic performance on biomimetic superhydrophobic surfaces and the effect of wettability and surface energy. *Appl. Surf. Sci.* **2019**, *466*, 503–514.
129. Cui, W.; Pakkanen, T.A. Icephobic performance of one-step silicone-oil-infused slippery coatings: Effects of surface energy, oil and nanoparticle contents. *J. Colloid Interface Sci.* **2019**, *558*, 251–258.
130. Farhadi, S.; Farzaneh, M.; Kulinich, S.A. Anti-icing performance of superhydrophobic surfaces. *Appl. Surf. Sci.* **2011**, *257*, 6264–6269.
131. Gao, J.; Zhang, Y.; Wei, W.; Yin, Y.; Liu, M.; Guo, H.; Zheng, C.; Deng, P. Liquid-infused micro-nanostructured MOF coatings (LIMNSMCs) with high anti-icing performance. *ACS Appl. Mater. Interfaces* **2019**, *11*, 47545–47552.
132. Gao, S.; Liu, B.; Peng, J.; Zhu, K.; Zhao, Y.; Li, X.; Yuan, X. Icephobic durability of branched PDMS slippage coatings co-cross-linked by functionalized POSS. *ACS Appl. Mater. Interfaces* **2019**, *11*, 4654–4666.
133. Ghalmi, Z.; Farzaneh, M. Experimental investigation to evaluate the effect of PTFE nanostructured roughness on ice adhesion strength. *Cold Reg. Sci. Technol.* **2015**, *115*, 42–47.
134. Gu, W.C.; Song, K.X.; Cheng, Z.; Wang, Q.L.; Wang, S.L.; Wang, X.K.; Yu, X.Q.; Zhang, Y.F. Water-based robust transparent superamphiphobic coatings for resistance to condensation, frosting, icing, and fouling. *Adv. Mater. Interfaces* **2020**, *7*, 1902201.
135. Guerin, F.; Laforte, C.; Farinas, M.I.; Perron, J. Analytical model based on experimental data of centrifuge ice adhesion tests with different substrates. *Cold Reg. Sci. Technol.* **2016**, *121*, 93–99.
136. Momen, G.; Farzaneh, M. Facile approach in the development of icephobic hierarchically textured coatings as corrosion barrier. *Appl. Surf. Sci.* **2014**, *299*, 41–46.
137. Menini, R.; Ghalmi, Z.; Farzaneh, M. Highly resistant icephobic coatings on aluminum alloys. *Cold Reg. Sci. Technol.* **2011**, *65*, 65–69.
138. He, Y.; Jiang, C.; Cao, X.; Chen, J.; Tian, W.; Yuan, W. Reducing ice adhesion by hierarchical micro-nano-pillars. *Appl. Surf. Sci.* **2014**, *305*, 589–595.
139. He, Z.; Wu, C.; Hua, M.; Wu, S.; Wu, D.; Zhu, X.; Wang, J.; He, X. Bioinspired multifunctional anti-icing hydrogel. *Matter* **2020**, *2*, 723–734.
140. He, Z.; Zhuo, Y.; Wang, F.; He, J.; Zhang, Z. Understanding the role of hollow sub-surface structures in reducing ice adhesion strength. *Soft Matter* **2019**, *15*, 2905–2910.

141. Hong, S.; Wang, R.; Huang, X.; Liu, H. Facile one-step fabrication of PHC/PDMS anti-icing coatings with mechanical properties and good durability. *Prog. Org. Coat.* **2019**, *135*, 263–269.
142. Idriss, H.; Guselnikova, O.; Postnikov, P.S.; Kolska, Z.; Haušild, P.; Čech, J.; Lyutakov, O.; Švorčík, V. Versatile and scalable icephobization of airspace composite by surface morphology and chemistry tuning. *ACS Appl. Polym. Mater.* **2020**, *2*, 977–986.
143. Irajizad, P.; Al-Bayati, A.; Eslami, B.; Shafquat, T.; Nazari, M.; Jafari, P.; Kashyap, V.; Masoudi, A.; Araya, D.; Ghasemi, H. Stress-localized durable icephobic surfaces. *Mater. Horiz.* **2019**, *6*, 758–766.
144. Jafari, R.; Menini, R.; Farzaneh, M. Superhydrophobic and icephobic surfaces prepared by RF-sputtered polytetrafluoroethylene coatings. *Appl. Surf. Sci.* **2010**, *257*, 1540–1543.
145. Jafari, R.; Momen, G.; Eslami, E. Fabrication of icephobic aluminium surfaces by atmospheric plasma jet polymerisation. *Surf. Eng.* **2018**, *35*, 450–455.
146. Jamil, M.I.; Zhan, X.; Chen, F.; Cheng, D.-G.; Zhang, Q. Durable and scalable candle soot icephobic coating with nucleation and fracture mechanism. *ACS Appl. Mater. Interfaces* **2019**, *11*, 31532–31542.
147. Jeon, J.; Jang, H.; Chang, J.; Lee, K.-S.; Kim, D.R. Fabrication of micro-patterned aluminum surfaces for low ice adhesion strength. *Appl. Surf. Sci.* **2018**, *440*, 643–650.
148. Jiang, G.; Chen, L.; Zhang, S.; Huang, H. Superhydrophobic SiC/CNTs coatings with photothermal deicing and passive anti-icing properties. *ACS Appl. Mater. Interfaces* **2018**, *10*, 36505–36511.
149. Jin, M.; Shen, Y.; Luo, X.; Tao, J.; Xie, Y.; Chen, H.; Wu, Y. A combination structure of microblock and nanohair fabricated by chemical etching for excellent water repellency and icephobicity. *Appl. Surf. Sci.* **2018**, *455*, 883–890.
150. Juuti, P.; Haapanen, J.; Stenroos, C.; Niemelä-Anttonen, H.; Harra, J.; Koivuluoto, H.; Teisala, H.; Lahti, J.; Tuominen, M.; Kuusipalo, J.; et al. Achieving a slippery, liquid-infused porous surface with anti-icing properties by direct deposition of flame synthesized aerosol nanoparticles on a thermally fragile substrate. *Appl. Phys. Lett.* **2017**, *110*, 161603.
151. Kim, A.; Kim, S.; Huh, M.; Kim, H.; Lee, C. Superior anti-icing strategy by combined sustainable liquid repellence and electro/photo-responsive thermogenesis of oil/MWNT composite. *J. Mater. Sci. Technol.* **2020**, *49*, 106–116.
152. Kim, P.; Wong, T.-S.; Alvarenga, J.; Kreder, M.J.; Adorno-Martinez, W.E.; Aizenberg, J. Liquid-infused nanostructured surfaces with extreme anti-ice and anti-frost performance. *ACS Nano* **2012**, *6*, 6569–6577.
153. Koivuluoto, H.; Hartikainen, E.; Niemelä-Anttonen, H. Thermally sprayed coatings: Novel surface engineering strategy towards icephobic solutions. *Materials* **2020**, *13*, 1434.
154. Koivuluoto, H.; Stenroos, C.; Kylmälahti, M.; Apostol, M.; Kiilakoski, J.; Vuoristo, P. Anti-icing behavior of thermally sprayed polymer coatings. *J. Therm. Spray Techn.* **2017**, *26*, 150–160.
155. Koshio, K.; Waku, T.; Hagiwara, Y. Ice-phobic glass-substrate surfaces coated with polypeptides inspired by antifreeze protein. *Int. J. Refrig.* **2020**, *114*, 201–209.
156. Kulinich, S.A.; Farhadi, S.; Nose, K.; Du, X.W. Superhydrophobic surfaces: Are they really ice-repellent? *Langmuir* **2011**, *27*, 25–29.
157. Kulinich, S.A.; Farzaneh, M. How wetting hysteresis influences ice adhesion strength on superhydrophobic surfaces. *Langmuir* **2009**, *25*, 8854–8856.
158. Kulinich, S.A.; Farzaneh, M. Ice adhesion on super-hydrophobic surfaces. *Appl. Surf. Sci.* **2009**, *255*, 8153–8157.
159. Kulinich, S.A.; Farzaneh, M. On ice-releasing properties of rough hydrophobic coatings. *Cold Reg. Sci. Technol.* **2011**, *65*, 60–64.
160. Kulinich, S.A.; Honda, M.; Zhu, A.L.; Rozhin, A.G.; Du, X.W. The icephobic performance of alkyl-grafted aluminum surfaces. *Soft Matter* **2015**, *11*, 856–861.
161. Li, H.; Li, X.; Luo, C.; Zhao, Y.; Yuan, X. Icephobicity of polydimethylsiloxane-b-poly(fluorinated acrylate). *Thin Solid Films* **2014**, *573*, 67–73.
162. Li, T.; Zhuo, Y.; Håkonsen, V.; Rønneberg, S.; He, J.; Zhang, Z. Epidermal gland inspired self-repairing slippery lubricant-infused porous coatings with durable low ice adhesion. *Coatings* **2019**, *9*, 602.
163. Li, X.; Li, Y.; Ren, L.; Zhu, K.; Zhao, Y.; Yuan, X. Self-crosslinking coatings of fluorinated polysiloxanes with enhanced icephobicity. *Thin Solid Films* **2017**, *639*, 113–122.
164. Li, X.; Wang, G.; Sofia Moita, A.; Zhang, C.; Wang, S.; Liu, Y. Fabrication of bio-inspired non-fluorinated superhydrophobic surfaces with anti-icing property and its wettability transformation analysis. *Appl. Surf. Sci.* **2019**, *505*, 144386.
165. Li, X.; Zhang, K.; Zhao, Y.; Zhu, K.; Yuan, X. Formation of icephobic film from POSS-containing fluorosilicone multi-block methacrylate copolymers. *Prog. Org. Coat.* **2015**, *89*, 150–159.
166. Li, X.; Zhang, K.; Zhao, Y.; Zhu, K.; Yuan, X. Enhancement of icephobic properties based on UV-curable fluorosilicone copolymer films. *RSC Adv.* **2015**, *5*, 90578–90587.
167. Li, X.; Zhao, Y.; Li, H.; Yuan, X. Preparation and icephobic properties of polymethyltrifluoropropylsiloxane–polyacrylate block copolymers. *Appl. Surf. Sci.* **2014**, *316*, 222–231.
168. Li, X.; Wang, G.; Zhan, B.; Li, S.; Han, Z.; Liu, Y. A novel icephobic strategy: The fabrication of biomimetic coupling micropatterns of superwetting surface. *Adv. Mater. Interfaces* **2019**, *6*, 1900864.
169. Li, Y.; Luo, C.; Li, X.; Zhang, K.; Zhao, Y.; Zhu, K.; Yuan, X. Submicron/nano-structured icephobic surfaces made from fluorinated polymethylsiloxane and octavinyl-POSS. *Appl. Surf. Sci.* **2016**, *360*, 113–120.
170. Ling, E.J.Y.; Uong, V.; Renault-Crispo, J.-S.; Kietzig, A.-M.; Servio, P. Reducing ice adhesion on nonsmooth metallic surfaces: Wettability and topography effects. *ACS Appl. Mater. Interfaces* **2016**, *8*, 8789–8800.
171. Liu, F.; Pan, Q. Facile fabrication of robust ice-phobic polyurethane sponges. *Adv. Mater. Interfaces* **2015**, *2*, 1500219.

172. Liu, F.; Wang, Z.; Pan, Q. Intelligent icephobic surface towards self-deicing capability. *ACS Sustain. Chem. Eng.* **2019**, *8*, 792–799.
173. Liu, G.; Yuan, Y.; Jiang, Z.; Youdong, J.; Liang, W. Anti-frosting/anti-icing property of nano-ZnO superhydrophobic surface on Al alloy prepared by radio frequency magnetron sputtering. *Mater. Res. Express* **2020**, *7*, 026401.
174. Liu, J.; Janjua, Z.; Roe, M.; Xu, F.; Turnbull, B.; Choi, K.-S.; Hou, X. Super-hydrophobic/icephobic coatings based on silica nanoparticles modified by self-assembled monolayers. *Nanomaterials* **2016**, *6*, 232.
175. Liu, J.; Wang, J.; Mazzola, L.; Memon, H.; Barman, T.; Turnbull, B.; Mingione, G.; Choi, K.-S.; Hou, X. Development and evaluation of poly(dimethylsiloxane) based composite coatings for icephobic applications. *Surf. Coat. Technol.* **2018**, *349*, 980–985.
176. Liu, M.; Ru, Y.; Fang, R.; Gu, Z.; Jiang, L. Reversibly thermosecreting organogels with switchable lubrication and anti-icing performance. *Angew. Chem. Int. Ed.* **2020**, *59*, 11876–11880.
177. Liu, Q.; Yang, Y.; Huang, M.; Zhou, Y.; Liu, Y.; Liang, X. Durability of a lubricant-infused electrospray silicon rubber surface as an anti-icing coating. *Appl. Surf. Sci.* **2015**, *346*, 68–76.
178. Liu, W.; Chen, H.; Shen, Y.; Wu, Z. Facilely fabricating superhydrophobic resin-based coatings with lower water freezing temperature and ice adhesion for anti-icing application. *J. Bionic Eng.* **2019**, *16*, 794–805.
179. Liu, X.; Chen, H.; Zhao, Z.; Yan, Y.; Zhang, D. Slippery liquid-infused porous electric heating coating for anti-icing and de-icing applications. *Surf. Coat. Technol.* **2019**, *374*, 889–896.
180. Liu, Y.; Ma, L.; Wang, W.; Kota, A.K.; Hu, H. An experimental study on soft PDMS materials for aircraft icing mitigation. *Appl. Surf. Sci.* **2018**, *447*, 599–609.
181. Liu, Y.; Tian, Y.; Chen, J.; Gu, H.; Liu, J.; Wang, R.; Zhang, B.; Zhang, H.; Zhang, Q. Design and preparation of bioinspired slippery liquid-infused porous surfaces with anti-icing performance via delayed phase inversion process. *Colloid Surface. A* **2020**, *588*, 124384.
182. Liu, Y.; Wang, C.; Jarrell, R.; Nair, S.S.; Wynne, K.J.; Di, D. Icephobic, Pt-cured, polydimethylsiloxane nanocomposite coatings. *ACS Appl. Mater. Interfaces* **2020**, *12*, 11180–11189.
183. Liu, Y.; Zhang, Z.; Hu, H.; Hu, H.; Samanta, A.; Wang, Q.; Ding, H. An experimental study to characterize a surface treated with a novel laser surface texturing technique: Water repellency and reduced ice adhesion. *Surf. Coat. Technol.* **2019**, *374*, 634–644.
184. Memon, H.; Liu, J.; De Focatiis, D.S.A.; Choi, K.S.; Hou, X. Intrinsic dependence of ice adhesion strength on surface roughness. *Surf. Coat. Technol.* **2020**, *385*, 125382.
185. He, Z.; Zhuo, Y.; Wang, F.; He, J.; Zhang, Z. Design and preparation of icephobic PDMS-based coatings by introducing an aqueous lubricating layer and macro-crack initiators at the ice-substrate interface. *Prog. Org. Coat.* **2020**, *147*, 105737.
186. Yao, H.; Gao, H. Gibson-soil-like materials achieve flaw-tolerant adhesion. *J. Comput. Theor. Nanos.* **2010**, *7*, 1299–1305.
187. Nosonovsky, M.; Hejazi, V. Why superhydrophobic surfaces are not always icephobic. *ACS Nano* **2012**, *6*, 8488–8491.
188. Viswanathan, K.; Sundaram, N.K.; Chandrasekar, S. Stick-slip at soft adhesive interfaces mediated by slow frictional waves. *Soft Matter* **2016**, *12*, 5265–5275.
189. Chaudhury, M.K.; Kim, K.H. Shear-induced adhesive failure of a rigid slabin contact with a thin confined film. *Eur. Phys. J. E* **2007**, *23*, 175–183.
190. Chaudhury, M.K.; Chakrabarti, A.; Ghatak, A. Adhesion-induced instabilities and pattern formation in thin films of elastomers and gels. *Eur. Phys. J. E* **2015**, *38*, 82.
191. Kendall, K. The adhesion and surface energy of elastic solids. *J. Phys. D Appl. Phys.* **1971**, *4*, 1186–1195.
192. Kumar, A.; Gupta, R.K. *Fundamentals of Polymer Engineering*, 3rd ed.; CRC Press: Boca Raton, FL, USA, 2003.
193. Morelle, X.P.; Illeperuma, W.R.; Tian, K.; Bai, R.; Suo, Z.; Vlassak, J.J. Highly stretchable and tough hydrogels below water freezing temperature. *Adv. Mater.* **2018**, *30*, 1801541.
194. Zhuo, Y.; Xiao, S.; Håkonsen, V.; He, J.; Zhang, Z. Anti-icing ionogel surfaces: Inhibiting ice nucleation, growth, and adhesion. *ACS Mater. Lett.* **2020**, *2*, 616–623.
195. He, Z.; He, J.; Zhang, Z. Selective growth of metallic nanostructures on microstructured copper substrate in solution. *CrystEngComm* **2015**, *17*, 7262–7269.
196. Zhang, H.Y.; Yang, Y.L.; Pan, J.F.; Long, H.; Huang, L.S.; Zhang, X.K. Compare study between icephobicity and superhydrophobicity. *Phys. B Condens. Matter* **2019**, *556*, 118–130.
197. He, Z.; Zhang, Z.; He, J. CuO/Cu based superhydrophobic and self-cleaning surfaces. *Scr. Mater.* **2016**, *118*, 60–64.
198. Cheng, Y.-T.; Rodak, D.E. Is the lotus leaf superhydrophobic? *Appl. Phys. Lett.* **2005**, *86*, 144101.
199. Papadopoulos, P.; Mammen, L.; Deng, X.; Vollmer, D.; Butt, H.-J. How superhydrophobicity breaks down. *Proc. Natl. Acad. Sci. USA* **2013**, *110*, 3254–3258.
200. Tang, Y.; Yang, X.; Li, Y.; Lu, Y.; Zhu, D. Robust micro-nanostructured superhydrophobic surfaces for long-term dropwise condensation. *Nano Lett.* **2021**, DOI: 10.1021/acs.nanolett.1c01584.
201. Ezazi, M.; Shrestha, B.; Klein, N.; Lee, D.H.; Seo, S.; Kwon, G. Self-healable superomniphobic surfaces for corrosion protection. *ACS Appl. Mater. Interfaces* **2019**, *11*, 30240–30246.
202. Zhang, H. Concrete. In *Building Materials in Civil Engineering*; Woodhead Publishing: Beijing, China, 2011; pp. 81–423.
203. Cao, L.; Jones, A.K.; Sikka, V.K.; Wu, J.; Gao, D. Anti-icing superhydrophobic coatings. *Langmuir* **2009**, *25*, 12444–12448.
204. Boinovich, L.B.; Emelyanenko, A.M.; Ivanov, V.K.; Pashinin, A.S. Durable icephobic coating for stainless steel. *ACS Appl. Mater. Interfaces* **2013**, *5*, 2549–2554.
205. Boinovich, L.B.; Emelyanenko, A.M.; Emelyanenko, K.A.; Modin, E.B. Modus operandi of protective and anti-icing mechanisms underlying the design of longstanding outdoor icephobic coatings. *ACS Nano* **2019**, *13*, 4335–4346.

206. Wang, L.; Gong, Q.; Zhan, S.; Jiang, L.; Zheng, Y. Robust anti-icing performance of a flexible superhydrophobic surface. *Adv. Mater.* **2016**, *28*, 7729–7735.
207. Vasileiou, T.; Schutzius, T.M.; Poulikakos, D. Imparting icephobicity with substrate flexibility. *Langmuir* **2017**, *33*, 6708–6718.
208. Wang, M.; Yu, W.; Zhang, Y.; Woo, J.-Y.; Chen, Y.; Wang, B.; Yun, Y.; Liu, G.; Lee, J.K.; Wang, L. A novel flexible micro-ratchet/ZnO nano-rods surface with rapid recovery icephobic performance. *J. Ind. Eng. Chem.* **2018**, *62*, 52–57.
209. Wong, T.-S.; Kang, S.H.; Tang, S.K.Y.; Smythe, E.J.; Hatton, B.D.; Grinthal, A.; Aizenberg, J. Bioinspired self-repairing slippery surfaces with pressure-stable omniphobicity. *Nature* **2011**, *477*, 443–447.
210. Han, L.; Zhao, X.; Kidalla, J.E. An investigation into the anti-icing properties of fabrics used for the outer layer of firefighter clothing. *Text. Res. J.* **2018**, *89*, 1500–1511.
211. Wang, N.; Xiong, D.; Lu, Y.; Pan, S.; Wang, K.; Deng, Y.; Shi, Y. Design and fabrication of the lyophobic slippery surface and its application in anti-icing. *J. Phys. Chem. C* **2016**, *120*, 11054–11059.
212. Stamatopoulos, C.; Hemrle, J.; Wang, D.; Poulikakos, D. Exceptional anti-icing performance of self-impregnating slippery surfaces. *ACS Appl. Mater. Interfaces* **2017**, *9*, 10233–10242.
213. Wang, N.; Xiong, D.; Pan, S.; Wang, K.; Shi, Y.; Deng, Y. Robust superhydrophobic coating and the anti-icing properties of its lubricants-infused-composite surface under condensing condition. *New J. Chem.* **2017**, *41*, 1846–1853.
214. Sun, J.; Wang, C.; Song, J.; Huang, L.; Sun, Y.; Liu, Z.; Zhao, C.; Li, Y. Multi-functional application of oil-infused slippery Al surface: From anti-icing to corrosion resistance. *J. Mater. Sci* **2018**, *53*, 16099–16109.
215. Niemelä-Anttonen, H.; Koivuluoto, H.; Tuominen, M.; Teisala, H.; Juuti, P.; Haapanen, J.; Harra, J.; Stenroos, C.; Lahti, J.; Kuusipalo, J.; et al. Icephobicity of slippery liquid infused porous surfaces under multiple freeze-thaw and ice accretion-detachment cycles. *Adv. Mater. Interfaces* **2018**, *5*, 1800828.
216. Metya, A.K.; Singh, J.K. Ice adhesion mechanism on lubricant-impregnated surfaces using molecular dynamics simulations. *Mol. Simulat.* **2018**, *45*, 1–9.
217. Alcaire, M.; Lopez-Santos, C.; Aparicio, F.J.; Sanchez-Valencia, J.R.; Obrero, J.M.; Saghi, Z.; Rico, V.J.; De la Fuente, X.; Gonzalez-Elipe, A.R.; Barranco, A.; et al. 3D organic nanofabrics: Plasma-assisted synthesis and anti-freezing behavior of superhydrophobic and lubricant-infused slippery surfaces. *Langmuir* **2019**, *35*, 16876–16885.
218. Gao, X.; Wen, G.; Guo, Z. Superhydrophobic and slippery cotton fabrics with robust nanolayers for stable wettability, anti-fouling and anti-icing properties. *New J. Chem.* **2019**, *43*, 16656–16663.
219. Guo, Z.; Gao, C.; Li, J.; Liu, Y.; Zheng, Y. Anti-icing properties of bioinspired liquid-infused double-layer surface with internal wetting transport ability. *Adv. Mater. Interfaces* **2019**, *6*, 1900244.
220. Liu, C.; Li, Y.; Lu, C.; Liu, Y.; Feng, S.; Liu, Y. Robust slippery liquid-infused porous network surfaces for enhanced anti-/de-icing performance. *ACS Appl. Mater. Interfaces* **2020**, *12*, 25471–25477.
221. Preston, D.J.; Song, Y.; Lu, Z.; Antao, D.S.; Wang, E.N. Design of lubricant infused surfaces. *ACS Appl. Mater. Interfaces* **2017**, *9*, 42383–42392.
222. Peppou-Chapman, S.; Hong, J.K.; Waterhouse, A.; Neto, C. Life and death of liquid-infused surfaces: A review on the choice, analysis and fate of the infused liquid layer. *Chem. Soc. Rev.* **2020**, *49*, 3688–3715.
223. Subramanyam, S.B.; Rykaczewski, K.; Varanasi, K.K. Ice adhesion on lubricant-impregnated textured surfaces. *Langmuir* **2013**, *29*, 13414–13418.
224. Rykaczewski, K.; Anand, S.; Subramanyam, S.B.; Varanasi, K.K. Mechanism of frost formation on lubricant-impregnated surfaces. *Langmuir* **2013**, *29*, 5230–5238.
225. Pang, H.; Zhou, S.; Gu, G.; Wu, L. Long-term hydrophobicity and ice adhesion strength of latex paints containing silicone oil microcapsules. *J. Adhes. Sci. Technol.* **2012**, *27*, 46–57.
226. Tao, C.; Li, X.; Liu, B.; Zhang, K.; Zhao, Y.; Zhu, K.; Yuan, X. Highly icephobic properties on slippery surfaces formed from polysiloxane and fluorinated POSS. *Prog. Org. Coat.* **2017**, *103*, 48–59.
227. Yeong, Y.H.; Milionis, A.; Loth, E.; Sokhey, J. Self-lubricating icephobic elastomer coating (SLIC) for ultralow ice adhesion with enhanced durability. *Cold Reg. Sci. Technol.* **2018**, *148*, 29–37.
228. Xiao, S.; He, J.; Zhang, Z. Nanoscale deicing by molecular dynamics simulation. *Nanoscale* **2016**, *8*, 14625–14632.
229. Rosenberg, R. Why is ice slippery? *Phys. Today* **2005**, *58*, 50–54.
230. Ozbay, S.; Yuceel, C.; Erbil, H.Y. Improved icephobic properties on surfaces with a hydrophilic lubricating liquid. *ACS Appl. Mater. Interfaces* **2015**, *7*, 22067–22077.
231. Zhao, T.Y.; Jones, P.R.; Patankar, N.A. Thermodynamics of sustaining liquid water within rough icephobic surfaces to achieve ultra-low ice adhesion. *Sci. Rep.* **2019**, *9*, 258.
232. Fletcher, N.H. Surface structure of water and ice. *Phil. Mag.* **1968**, *18*, 1287–1300.
233. Döppenschmidt, A.; Kappl, M.; Butt, H.-J. Surface properties of ice studied by atomic force microscopy. *J. Phys. Chem. B* **1998**, *102*, 7813–7819.
234. Wettlaufer, J.S. Impurity effects in the premelting of ice. *Phys. Rev. Lett.* **1999**, *82*, 2516–2519.
235. Ikeda-Fukazawa, T.; Kawamura, K. Molecular-dynamics studies of surface of ice Ih. *J. Chem. Phys.* **2004**, *120*, 1395–1401.
236. Menini, R.; Farzaneh, M. Advanced icephobic coatings. *J. Adhes. Sci. Technol.* **2011**, *25*, 971–992.
237. Li, C.; Li, X.; Tao, C.; Ren, L.; Zhao, Y.; Bai, S.; Yuan, X. Amphiphilic antifogging/anti-icing coatings containing POSS-PDMAEMA-b-PSBMA. *ACS Appl. Mater. Interfaces* **2017**, *9*, 22959–22969.

238. Zigmond, J.S.; Pavía-Sanders, A.; Russell, J.D.; Wooley, K.L. Dynamic anti-icing coatings: Complex, amphiphilic hyperbranched fluoropolymer poly(ethylene glycol) cross-linked networks with an integrated liquid crystalline comonomer. *Chem. Mater.* **2016**, *28*, 5471–5479.
239. Koshio, K.; Arai, K.; Waku, T.; Wilson, P.W.; Hagiwara, Y. Suppression of droplets freezing on glass surfaces on which antifreeze polypeptides are adhered by a silane coupling agent. *PLoS ONE* **2018**, *13*, e0204686.
240. Liu, Z.; He, Z.; Lv, J.; Jin, Y.; Wu, S.; Liu, G.; Zhou, F.; Wang, J. Ion-specific ice propagation behavior on polyelectrolyte brush surfaces. *RSC Adv.* **2017**, *7*, 840–844.
241. Ezzat, M.; Huang, C.-J. Zwitterionic polymer brush coatings with excellent anti-fog and anti-frost properties. *RSC Adv.* **2016**, *6*, 61695–61702.
242. Tao, C.; Bai, S.; Li, X.; Li, C.; Ren, L.; Zhao, Y.; Yuan, X. Formation of zwitterionic coatings with an aqueous lubricating layer for antifogging/anti-icing applications. *Prog. Org. Coat.* **2018**, *115*, 56–64.
243. Lee, H.; Alcaraz, M.L.; Rubner, M.F.; Cohen, R.E. Zwitter-wettability and antifogging coatings with frost-resisting capabilities. *ACS Nano* **2013**, *7*, 2172–2185.
244. Liang, B.; Zhang, G.; Zhong, Z.; Huang, Y.; Su, Z. Superhydrophilic anti-icing coatings based on polyzwitterion brushes. *Langmuir* **2019**, *35*, 1294–1301.
245. Li, T.; Ibáñez Ibáñez, P.F.; Håkonsen, V.; Wu, J.; Xu, K.; Zhuo, Y.; Luo, S.; He, J.; Zhang, Z. Self-deicing electrolyte hydrogel surfaces with Pa-level ice adhesion and durable anti-freezing/frost performance. *ACS Appl. Mater. Interfaces* **2020**, *12*, 35572–35578.
246. Xu, X.; Jerca, V.V.; Hoogenboom, R. Bio-inspired hydrogels as multi-task anti-icing hydrogel coatings. *Chem* **2020**, *6*, 808–831.
247. Chen, T.K.; Cong, Q.; Li, Y.; Jin, J.F.; Choy, K.L. Utilizing swelling force to decrease the ice adhesion strength. *Cold Reg. Sci. Technol.* **2018**, *146*, 122–126.
248. Chen, T.; Jin, J.; Qi, Y.; Tian, W.; Cong, Q.; Choy, K.-L. Disturbing stability of interface by adopting phase-change temperature gradient to reduce ice adhesion strength. *Cold Reg. Sci. Technol.* **2019**, *158*, 69–75.
249. Irajizad, P.; Hasnain, M.; Farokhnia, N.; Sajadi, S.M.; Ghasemi, H. Magnetic slippery extreme icephobic surfaces. *Nat. Commun.* **2016**, *7*, 13395.
250. Lee, S.-H.; Seong, M.; Kwak, M.K.; Ko, H.; Kang, M.; Park, H.W.; Kang, S.M.; Jeong, H.E. Tunable multimodal drop bouncing dynamics and anti-icing performance of a magnetically responsive hair array. *ACS Nano* **2018**, *12*, 10693–10702.
251. Ma, L.; Wang, J.; Zhao, F.; Wu, D.; Huang, Y.; Zhang, D.; Zhang, Z.; Fu, W.; Li, X.; Fan, Y. Plasmon-mediated photothermal and superhydrophobic TiN-PTFE film for anti-icing/deicing applications. *Compos. Sci. Technol.* **2019**, *181*, 107696.
252. Wu, D.; Ma, L.; Zhang, F.; Qian, H.; Minhas, B.; Yang, Y.; Han, X.; Zhang, D. Durable deicing lubricant-infused surface with photothermally switchable hydrophobic/slippery property. *Mater. Des.* **2020**, *185*, 108236.
253. Jamil, M.I.; Wang, Q.; Ali, A.; Hussain, M.; Aziz, T.; Zhan, X.; Zhang, Q. Slippery photothermal trap for outstanding deicing surfaces. *J. Bionic Eng.* **2021**, *18*, 548–558.
254. Liu, Y.; Wu, Y.; Liu, Y.; Xu, R.; Liu, S.; Zhou, F. Robust photothermal coating strategy for efficient ice removal. *ACS Appl. Mater. Interfaces* **2020**, *12*, 46981–46990.
255. Hao, T.; Zhu, Z.; Yang, H.; He, Z.; Wang, J. All-day anti-icing/deicing film based on combined photo-electro-thermal conversion. *ACS Appl. Mater. Interfaces* **2021**, *13*, 44948–44955.
256. Wang, P.; Yao, T.; Li, Z.; Wei, W.; Xie, Q.; Duan, W.; Han, H. A superhydrophobic/electrothermal synergistically anti-icing strategy based on graphene composite. *Compos. Sci. Technol.* **2020**, *198*, 108307.
257. Harper, A.; Liu, G. Thickness of the ice-shedding lubricant layer in equilibrium with an underlying crosslinked polymer film. *ACS Appl. Polym. Mater.* **2020**, *2*, 1369–1377.
258. Wang, Z.; Zhu, Y.; Liu, X.; Zhao, Z.; Chen, J.; Jing, X.; Chen, H. Temperature self-regulating electrothermal pseudo-slippery surface for anti-icing. *Chem. Eng. J.* **2021**, *422*, 130110.